Continuous flow synthesis of a blocked polyisocyanate: process optimization and reaction monitoring by in-line FT-IR spectroscopy

Glotz, Gabriel

Master's thesis / Diplomski rad

2019

Degree Grantor / Ustanova koja je dodijelila akademski / stručni stupanj: **University of Zagreb, Faculty of Science / Sveučilište u Zagrebu, Prirodoslovno-matematički fakultet**

Permanent link / Trajna poveznica: https://urn.nsk.hr/urn:nbn:hr:217:284848

Rights / Prava: In copyright / Zaštićeno autorskim pravom.

Download date / Datum preuzimanja: **2024-08-01**

Repository / Repozitorij:

Repository of the Faculty of Science - University of Zagreb

University of Zagreb
FACULTY OF SCIENCE
Department of Chemistry

Gabriel Glotz

CONTINUOUS FLOW SYNTHESIS OF A BLOCKED POLYISOCYANATE: PROCESS OPTIMIZATION AND REACTION MONITORING BY *IN-LINE* FT-IR SPECTROSCOPY

Diploma Thesis

submitted to the Department of Chemistry,
Faculty of Science, University of Zagreb
for the academic degree of Master in Chemistry

Zagreb, 2019.

This Diploma Thesis was performed at the Center for Continuous Flow Synthesis and Processing, Institute of Chemistry, University of Graz, under the mentorship of Dr. Christian Oliver Kappe, Prof.

The supervisor appointed by the Department of Chemistry, Faculty of Science, University of Zagreb is Dr. Snežana Miljanić, Assoc. Prof.

Acknowledgments

I would like to gratefully acknowledge all the help I got from Dr. Christian Oliver Kappe, Prof. not just in producing this thesis but in all of my work so far in his group in Graz. In addition I thank Dr. David Cantillo for all of his help, and all of my colleagues in the Kappe laboratory in Graz.

Financial support from Allenx Austria GmbH and use of infrastructure of the COMET K project “Center for Continuous Flow Synthesis and Processing (Research Center Pharmaceutical Engineering GmbH and University of Graz) is also acknowledged.

Table of Contents

University of Zagreb
Faculty of Science
Department of Chemistry

Diploma Thesis

ABSTRACT

CONTINUOUS FLOW SYNTHESIS OF A BLOCKED POLYISOCYANATE: PROCESS OPTIMIZATION AND REACTION MONITORING BY *IN-LINE* FT-IR SPECTROSCOPY

Gabriel Glotz

Given that the traditional batch production of blocked isocyanates has significant drawbacks associated with the exothermic character of the reaction and the high viscosity of the materials involved, a continuous flow strategy was developed. The neat oxime and the viscous polyisocyanate were mixed using a Kenics® static mixer and the homogeneous mixture obtained was fully converted to the target blocked isocyanate in a residence time unit downstream of the mixer. Real-time reaction monitoring via *in-line* FT-IR spectroscopy at the reactor outlet has been implemented, enabling fast optimization of the reaction conditions and providing a sensitive and reliable control of the product quality. The process has been intensified by an increase in the flow rate of the reactants, a decrease in the residence unit volume and a stepwise increase in the temperature of the flow reactor. Full conversion to the blocked polyisocianate has been achieved at 155 °C after only 15 s of the overall residence time, providing productivity of ca. 1 kg per hour for a reactor of only 4.5 mL volume.

(43+XIX pages, 46 figures, 1 table, 97 references, original in English)

Thesis deposited in the Central Chemical Library, Faculty of Science, University of Zagreb, Horvatovac 102a, Zagreb, Croatia and in the Repository of the Faculty of Science, University of Zagreb

Keywords: blocked isocyanates, continuous-flow, continuous processing, *in-line* analytics, process optimization

Mentor: Dr. Christian Oliver Kappe, Professor
Supervisor: Dr. Snežana Miljanić, Associate Professor
Reviewers:
1. Dr. Snežana Miljanić, Associate Professor
2. Dr. Vesna Petrović Peroković, Associate Professor
3. Dr. Željka Soldin, Professor
Substitute: Dr. Ines Primožič, Professor
Date of exam: 08.04.2019.

Sveučilište u Zagrebu
Prirodoslovno-matematički fakultet
Kemijski odsjek

Diplomski rad

SAŽETAK

SINTEZA ZAŠTIĆENOG POLIIZOCIJANATA U KONTINUIRANOM PROTOKU: OPTIMIZACIJA PROCESA I PRAĆENJE REAKCIJE FT-IR SPEKTROSKOPIJOM *IN-LINE*

Gabriel Glotz

S obzirom da tradicionalna serijska proizvodnja zaštićenih izocijanata ima značajne nedostatke vezane uz egzotermni karakter reakcije i visoku viskoznost tvari koje sudjeluju u reakciji, razvijena je strategija sinteze u kontinuiranom protoku. Čisti oksim i viskozni poliizocijanat miješaju se pomoću statičke miješalice Kenics® te se dobivena homogena smjesa potpuno prevodi u ciljani zaštićeni izocijanat u protočnom reaktoru. Praćenje reakcije u realnom vremenu provedeno je FT-IR spektroskopijom *in-line* reakcijske smjese na izlasku iz reaktora, što je omogućilo brzu optimizaciju reakcijskih uvjeta te osiguralo osjetljivu i pouzdanu kontrolu kvalitete produkta. Proces je optimiziran povećanjem brzine protoka reaktanata, smjanjenjem volumena cijevnog reaktora te postupnim povećanjem temperature protočnog reaktora. Potpuna pretvorba u zaštićeni izocijanat postignuta je pri 155 °C nakon samo 15 s ukupnog vremena zadržavanja u reaktoru, čime je postignuta produktivnost od približno 1 kg na sat u reaktoru volumena od samo 4,5 mL.

(43+XIX stranica, 46 slika, 1 tablica, 97 literaturnih navoda, jezik izvornika: Engleski)

Rad je pohranjen u Središnjoj kemijskoj knjižnici Prirodoslovno-matematičkog fakulteta Sveučilišta u Zagrebu, Horvatovac 102a, Zagreb i Repozitoriju Prirodoslovno-matematičkog fakulteta Sveučilišta u Zagrebu

Ključne riječi: analitika *in-line,* kontinuirani process, kontinuirani protok, optimizacija procesa, zaštićeni izocijanati

Mentor: prof. dr. sc. Christian Oliver Kappe
Nastavnik: izv. prof. dr. sc. Snežana Miljanić
Ocjenitelji:
1. izv. prof. dr. sc. Snežana Miljanić
2. izv. prof. dr. sc. Vesna Petrović Peroković
3. prof. dr. sc. Željka Soldin
Zamjena: prof. dr. sc. Ines Primožič

Datum diplomskog ispita: 08.04.2019

PROŠIRENI SAŽETAK

Zbog velike potražnje za poliuretanima (godišnja proizvodnja iznad 5 milijuna tona samo u Europi), sinteza poliizocijanata i zaštićenih monomera iz kojih se pripravljaju poliuretani provodi se na velikoj skali. Reakcije kojima se zaštićuju izocijanati većinom su vrlo egzotermne.[I] Iz tog se razloga pri klasičnoj sintezi reagens za zaštitu dodaje postupno u reakcijsku smjesu uz kontinuiranu kontrolu temperature, što vrlo često ograničava produktivnost samog procesa.[II] Važan primjer je sinteza zaštićenog trimera heksametilendiizocijanata (engl. *blocked hexamethylene diisocyanate trimer,* B-HDIT) reakcijom trimera heksametilendiizocijanata (engl. *hexamethylene diisocyanate trimer*, HDIT) i etil-metil-ketoksima (engl. *methyl ethyl ketoxime,* MEKO). HDIT je komercijalno dostupan trimer heksametilendiizocijanata (HDI), (slika I), koji se često koristi u industriji zbog manje toksičnosti i hlapljivosti u odnosu na HDI, a ponajviše zbog svojstva umrežavanja polimera u proizvodnji poliuretana. Priprava B-HDIT-a provodi se na skali od desetak tona po šarži, pri čemu se MEKO postepeno dodaje u reaktor zbog egzotermne prirode reakcije. Elegantan način prevladavanja ograničenja trenutne proizvodnje zaštićenih izocijanata u klasičnom kotlastom reaktoru te osiguranja robustnosti procesa i konstantne kvalitete proizvoda jest sinteza u kontinuiranom protoku. Zahvaljujući učinkovitom prijenosu toplinske energije i miješanju reakcijske smjese, veoma egzotermne reakcije mogu se bez rizika provesti u protočnom reaktoru.[III–VI]

Do sada je u literaturi opisan samo jedan postupak sinteze zaštićenog poliizocijanata u kontinuiranom protoku.[IV] Prema protokolu koji je osmislio Cargill 1977. godine, reaktanti (poliizocijanat i reagens za zaštitu) unose se u reakcijsku zonu u odgovarajućem stehiometrijskom omjeru, iz koje se kontinuirano odvodi produkt.[IV]

I. Y. Camberlin, P. Michaud, C. Pesando, J. P. Pascault, *Makromol. Chem. Macromol. Symp.* **25** (1989) 91–99.
II. D. Levin, *ACS Symposium Series* **1181** (2014) 3–71.
III. M. B. Plutschack, B. Pieber, K. Gilmore, P. H. Seeberger, *Chem. Rev.* **117** (2017) 11796–11893.
IV. B. Gutmann, D. Cantillo, C. O. Kappe, *Angew. Chem. Int. Ed.* **54** (2015) 6688–6728.
V. I. R. Baxendale, L. Brocken, C. J. Mallia, *Green Proc. Synth.* **2** (2013) 211–230.
VI. E. L. Paul, V. A. Atiemo-Obeng, S. M. Kresta, *Handbook of Industrial Mixing: Science and Practice;* John Wiley & Sons, 2004; pp 1385.

VII. P. K. A. Panandiker, D. E. Tweet, *Continuous Process for the Production of Blocked Isocyanates*, U. S. Patent 4,055,551, 1977.

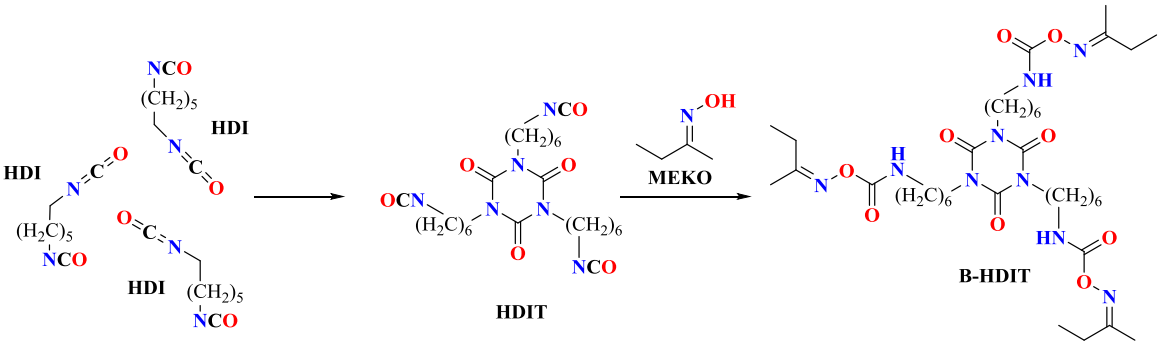

Slika I. Priprava trimera HDI (HDIT) i njegova zaštićenog derivata (B-HDIT) koristeći MEKO kao reagens za zaštitu.

U okviru ovog diplomskog rada istražit će se mogućnost sinteze zaštićenog izocijanata B-HDIT-a reakcijom trimernog izocijanata HDIT-a sa zaštitnim reagensom MEKO u protočnom reaktoru. U tu će se svrhu reakcija početno optimizirati klasičnom sintezom pri različitim temperaturama. Stabilnost produkta pri povišenim temperaturama utvrdit će se primjenom jednodimenzijske i dvodimenzijske infracrvene (IR) spektroskopije, spektroskopije NMR te razlikovne pretražne kalorimetrije (DSC). Nakon toga će se sinteza provoditi u protočnom reaktoru. S obzirom na visoku viskoznost HDIT-a pri sobnoj temperature (3000 mPa s), koja otežava miješanje reakcijske smjese, posebna pažnja posvetit će se sustavu za unos i miješanje reaktanata te izvedbi protočnog reaktora. Praćenje sinteze zaštićenog izocijanata u kontinuiranom protoku u realnom vremenu provest će se FT-IR spektroskopijom *in-line*.

U IR spektru trimernog izocijanata HDIT-a uočava se široka vrpca asimetričnog istezanja izocijanatne skupine (N=C=O), čija su dva vrha (2297 cm^{-1} i 2230 cm^{-1}) posljedica Fermijeve rezonancije. Intenzitet NCO vibracijske vrpce (apsorbancija pri 2261 cm^{-1}), karakteristične za HDIT, korišten je za kvantitativno određivanje trimernog izocijanata tijekom reakcije konverzije u zaštićeni derivat. U tu svrhu provedena je kalibracija pomoću serije pripravljenih smjesa reaktanta HDIT-a i produkta B-HDIT-a poznatih masenih udjela. S obzirom na jak intenzitet vrpce istezanja skupine N=C=O, u spektrima smjesa masenog udjela izocijanata w(HDIT) > 50 % opaženo je zasićenje detektora ($A \approx 1$) (slika IIa). Međutim, za smjese manjeg masenog udjela, w(HDIT) < 30 %, uočena je linearna ovisnost apsorbancije vibracijske vrpce (2261 cm^{-1}) o masenom udjelu izocijanata (slika IIb). Iako koncentraciju

HDIT-a nije bilo moguće odrediti na početku reakcije, količinu reaktanta bilo je moguće pratiti pri završetku reakcije. Nadalje, pomoću serije otopina HDIT-a pripravljenih u butyl-acetatu određene su granica detekcije i granica kvantifikacije HDIT-a. Kao otapalo korišten je butyl-acetat zbog niske viskoznosti pri sobnoj temperaturi i dobre topljivosti izocijanata. Granica detekcije HDIT-a iznosila je 7 mmol L^{-1}, a granica kvantifikacije 9,7 mmol L^{-1} (slika IIc).

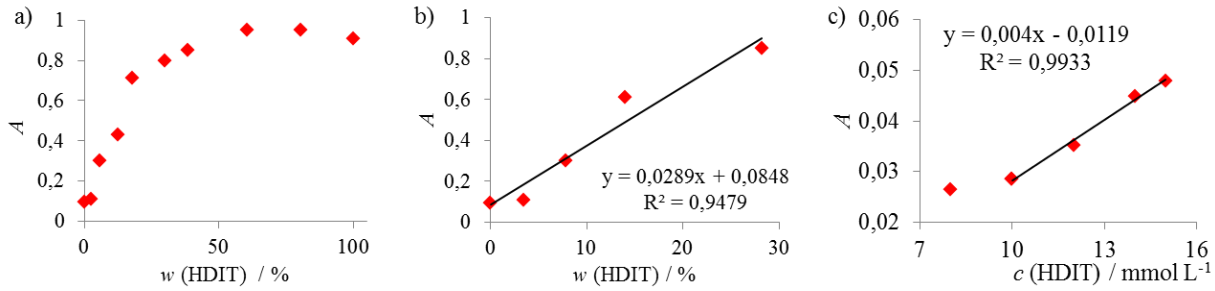

Slika II. Ovisnost apsorbancije IR vrpce izocijanata pri 2261 cm^{-1}: a) o masenom udjelu HDIT-a u smjesi s B-HDIT-om, *w*(HDIT) = 0–100 %; b) o masenom udjelu HIDT-a u smjesi s B-HDIT-om, *w*(HDIT) = 0–30 %; c) o koncentraciji HDIT-a u butil-acetatu, *c*(HDIT) = 7–15 mmol L^{-1} .

Stabilnost zaštićenog trimernog izocijanata B-HDIT-a pri povišenoj temperaturi istražena je razlikovnom pretražnom kalorimetrijom (DSC), jednodimenzijskom i dvodimenzijskom IR spektroskopijom te spektroskopijom NMR. Uzorak B-HDIT-a za DSC analizu (5 mg) zagrijavan je postupno od sobne temperature do 250 °C (5 °C min^{-1}) u struji dušika. U temperaturnom rasponu od 170 °C do 220 °C primijećen je široki endotermni signal.[VIII] Kako bi se utvrdilo upućuje li opaženi signal na raspad B-HDIT-a na HDIT i MEKO, a uzimajući u obzir činjenicu da se karakteristična vrpca izocijanata HDIT-a lako uočava u IR spektru, snimani su IR spektri uzorka B-HDIT-a tijekom zagrijavanja od sobne temperature do 160 °C (8 °C min^{-1}) u vremenskim razmacima od 15 s. Provedena je korelacijska analiza snimljenih IR spektara[IX] kako bi se u dvodimenzijskim korelacijskim IR spektrima (2D-IRcorr) uočile promjene intenziteta vrpci i pomaci vrpci koje je u jednodimenzijskim IR spektrima teže raspoznati. Sinhronizirani korelacijski spektar ukazao je na cijepanje vodikovih veza između skupine C=O karbamata kao akceptora vodikove veze (HBA) i skupine NH kao donora vodikove veze (HBD) koje je uzrokovano povišenjem temperature (slika III, crveni dvadrat). Nadalje, uzorak B-HDIT-a zagrijavan je pri 180 °C

tijekom 1 sata pri čemu su snimani IR spektri u vremenskim intervalima od 1 min. Snimljeni IR spektri također su korelirani. U 2D-IRcorr spektru nisu opažene značajne korelacije iznad razine šuma u spektru. Isti uzorak B-HDIT-a nakon zagrijavanja analiziran je spektroskopijom ^{1}H i ^{13}C NMR. Nije uočena razlika u NMR spektrima zagrijavanog uzorka i uzorka koji nije bio podvrgnut toplinskom stresu, što je potvrdilo stabilnost spoja u istraživanom temperaturnom području.

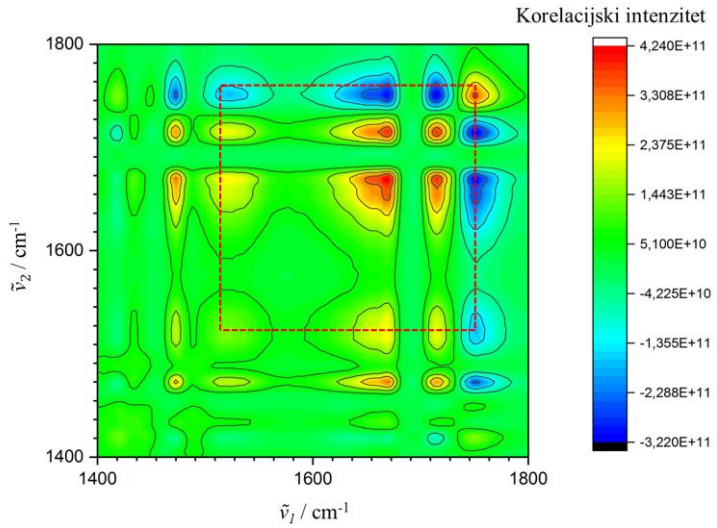

Slika III. Sinhronizirani 2D-IRcorr spektar B-HDITA tijekom zagrijavanja od sobne temperature do 160 °C u području valnih brojeva od 1800 cm^{-1} do 1400 cm^{-1}.

VIII. T. Shen, D. Zhou, L. Liang, J. Zheng, Y. Lan, M. Lu, *J. Appl. Polym. Sci.* **122** (2011) 748–757.

IX. I. Noda, Y. Liu, Y. Ozaki, *J. Phys. Chem.* **100** (1996) 8665–8673.

Početna optimizacija sinteze zaštićenog trimernog izocijanata B-HDIT-a reakcijom polaznog trimernog izocijanata HDIT-a mase 7 g (15 mmol) s reagensom za zaštitu MEKO, provedena je u okrugloj tikvici uz mehaničko miješanje. Reakcija je praćena FT-IR spektroskopijom pomoću sonde uronjene u reakcijsku smjesu u tikvici. Na početku reakcije u tikvici je bio samo HDIT pri sobnoj temperaturi ili zagrijan na odgovarajuću temperaturu, u koju je potom dodan MEKO. Tijek reakcije praćen je na temelju promjene intenziteta vibracijske vrpce izocijanatne skupine HDIT-a (2261 cm^{-1}). Istovremeno je praćena i temperatura reakcijske smjese pomoću senzora za mjerenje temperature smještenog u IR sondi. Reakcija je provedena pri temperaturama od 28 °C, 54 °C i 74 °C bez dodatka katalizatora, te pri temperaturi 28 °C uz dodatak katalizatora dibutil-kositarova dilaureata.

Tijekom svih navedenih sinteza opaženo je slabljenje intenziteta vrpce reaktanta HDIT-a pri 2261 cm^{-1}, koja naposljetku potpuno nestaje u vremenu kraćem od 2 min nakon dodatka reagensa za zaštitu (slika IV). Istovremeno, temperatura rekacijske smjese naglo raste.

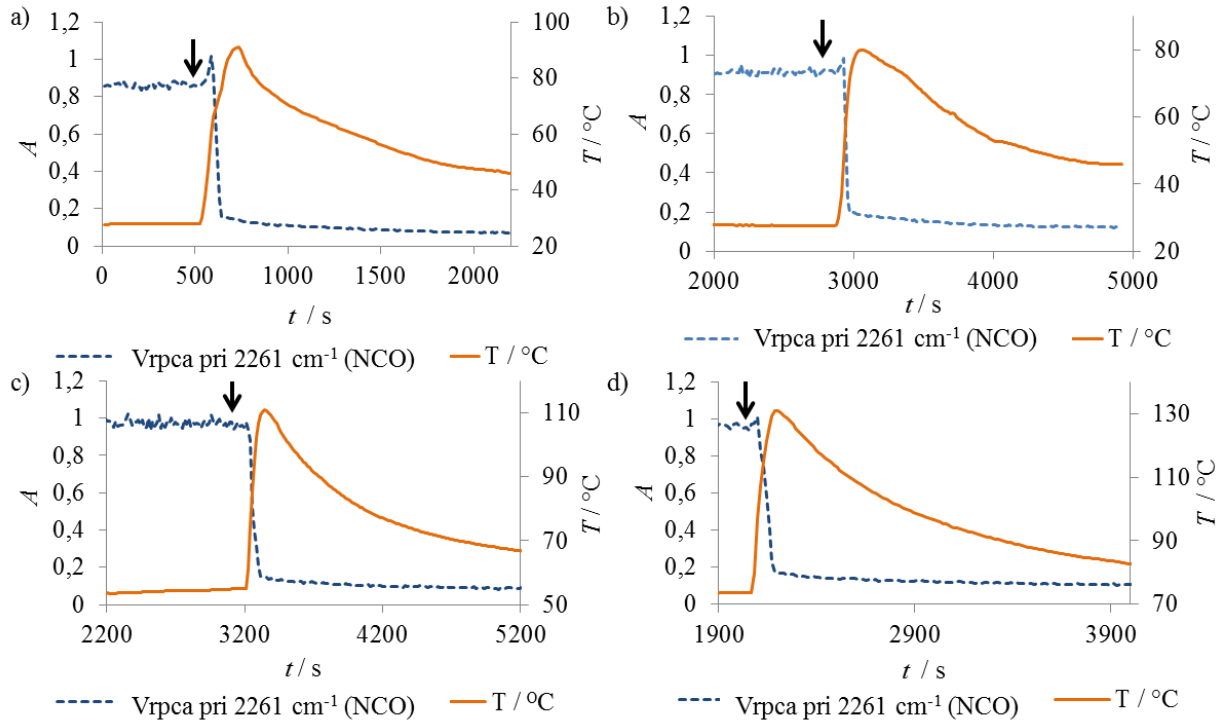

Slika IV. Praćenje tijeka reakcije HDIT-a I MEKO-a. Promjena intenziteta vrpce istezanja skupine N=C=O pri 2261 cm^{-1} i temperature reakcijske smjese tijekom reakcije HDIT-a i MEKO-a pri: a) 28 °C, b) 28 °C uz dodatak dibutil-kositrova dilaureata kao katalizatora, c) 54 °C i d) 74 °C. Trenutak u kojem je MEKO dodan u reakcijsku smjesu označen je strelicom.

Na slici IV opaža se da je reakcija HDIT-a s MEKO-m vrlo brza (< 2 min), dodatak katalizatora ne ubrzava je te je vrlo egzotermna. Sve to upućuje na mogućnost intenzifikacije sintetskog procesa koristeći protočni reaktor, koji je u tu svrhu dizajniran. Zbog visoke viskoznosti HDIT-a pri sobnoj temperaturi, koja otežava unos reaktanta u protočni reaktor na sobnoj temperaturi, trimerni izocijanat HDIT zagrije se na 75 °C i potom unosi u reaktor pomoću pumpe Vapourtec SF10. Za unos zaštitnog reagensa MEKO u protočni reaktor koristi se pumpa Syrris (slika Va). Reaktanti se dolaze u kontakt u modificiranom Y konektoru (slika Vc) na način da struja zaštitnog reagensa ulazi u centar struje trimernog izocijanata[X] i to netom prije unosa u statičku miješalicu Kenics (slika Vb). U miješalici se reaktanti gotovo

trenutno miješaju te se nastala homogena smjesa odvodi dalje u cijevni reaktor, koji je na željenu temperaturu zagrijan plaštom za grijanje kroz koji cirkulira silikonsko ulje. Na izlazu iz reaktora nalazi se modificirani T konektor iz kojeg reakcijska smjesa, kroz cjevčicu pod kutem od 90º izlazi van. Kratka cjevčica (2 cm) na izlazu iz reaktora sprječava brzo hlađenje nastalog produkta B-HDIT-a, koji bi s obzirom na visoku viskoznost pri sobnoj temperaturi mogao otežati i usporiti protok reakcijske smjese. U trećem otvoru T konektora pričvršćena je IR sonda, spojena s FT-IR spektrometrom.

Početna sinteza u protočnom reaktoru provedena je u cijevnom reaktoru volumena 14,65 mL pri temperaturi od 100 °C (V_2 i T_2 na slici Va), pri čemu temperatura miješalice Keniks (V_1 = 0,98 mL) nije bila kontrolirana. U takvoj postavi korištene su brzine protoka reaktanata od 1,00 mL min^{-1} za MEKO i 1,74 mL min^{-1} za HDIT, što je rezultiralo vremenom zadržavanja reakcijske smjese u reaktoru od 5,35 min, a tijekom kojeg je primijećena potpuna konverzija reaktanta HDIT-a u zaštićeni produkt B-HDIT. Zatim su uz nepromijenjeni volumen reaktora (V_2 = 14,65 mL) protoci reaktanata postepeno povećavani, od ukupnog protoka 2,74 mL min^{-1} do 14,10 mL min^{-1}, čime se vrijeme zadržavanja u reaktoru smanjilo s 5,35 min na 1,04 min. Tijekom ovih sinteza također je u potpunosti nastao zaštićeni izocijanat. Kako bi se dodatno skratilo vrijeme zadržavanja u reaktoru smanjen je volumen cijevnog reaktora (V_2 = 3,5 mL). Pri ukupnom protoku od 14,10 mL min^{-1}, vrijeme reakcije iznosilo je 45 s, ali uz nepotpunu konverziju u produkt pri kojoj je zaostalo 10 % neizreagiranog trimernog izocijanata.

X. J. Z. Luo, G. W. Chu, Y. Luo, M. Arowo, B. C. Sun, J. F. Chen, *AIChE J.* **63** (2017) 2876–2887.

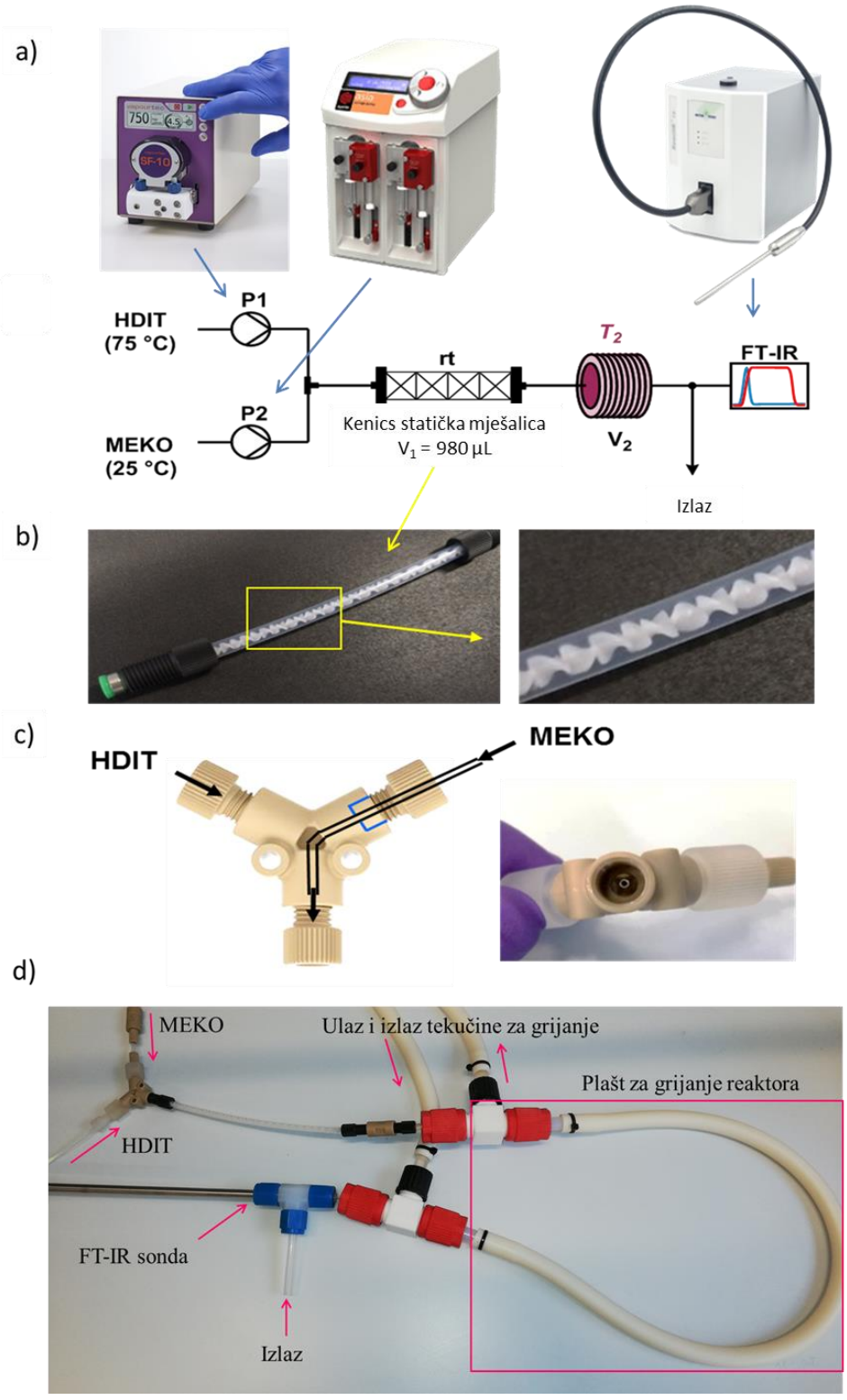

Slika V. Shematski i slikoviti prikaz dizajniranog protočnog reaktora i njegovih dijelova: a) shematski prikaz protočnog reaktora te fotografije korištenih pumpi i IR sonde, b) slikoviti prikaz statičke miješalice Kenics, c) shematski prikaz i slikoviti prikaz modificiranog Y konektora, d) slikoviti prikaz cijelog protočnog reaktora.

U svrhu optimizacije procesa korišten je ukupan protok za reaktante MEKO i HDIT od 14,10 mL min^{-1} te je temperatura cijevnog reaktora (slika Va) postupno povećavana od 100 °C do 155 °C. Potpuna konverzija u produkt primijećena je pri temperaturi od 155 °C i vremenu zadržavanja od 15 s (slika VI).

Temperatura reakcije od 155 °C i vrijeme zadržavanja reakcijske smjese u reaktoru od 15 s bili su uvjeti pri kojima je provjerena stabilnost procesa i reaktora tijekom vremena. U tu svrhu provedena je reakcija u trajanju od 3,5 sati praćena FT-IR spektroskopijom *in-line*. Promjena intenziteta vibracijske vrpca skupine N=C=O (2261 cm^{-1}) ukazala je na potpunu konverziju reaktanta u produkt (0 % NCO) pri navedenim uvjetima. Tijekom sinteze prikupljeno je 3,3 kg čistog B-HDIT-a, što odgovara produktivnosti od 1 kg h^{-1} za reaktor volumena 4,5 mL (unutarnji volumen statičke miješalice (V_1 = 0,98 mL) + volumen cijevnog reaktora (V_2 = 3,5 mL)).

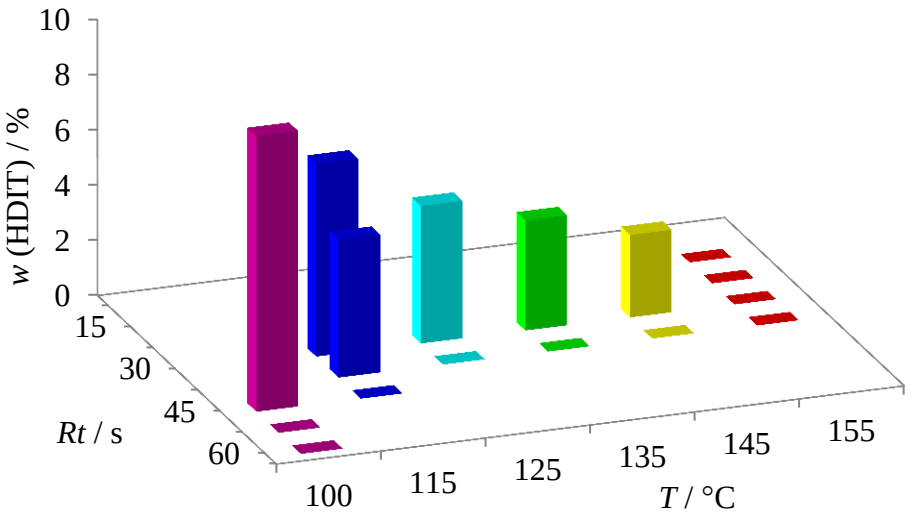

Slika VI. 3D prikaz konverzije reaktanta HDIT-a u produkt B-HDIT izražene preko ovisnosti masenog udjela preostalog HDIT-a o vremenu zadržavanja reakcijske smjese u reaktoru i temperaturi reaktora.

U ovom diplomskom radu dizajniran je protočni reaktor za sintezu zaštićenog poliizocijanata B-HDIT-a reakcijom trimernog izocijanata HDIT-a i zaštitnog reagensa MEKO-a. Optimizaciju uvjeta reakcije omogućila je FT-IR spektroskopija *in-line* praćenjem

promjene intenziteta vrpce asimetričnog istezanja izocijanatne skupine reaktanta HDIT-a (2261 cm^{-1}) tijekom reakcije. Opisani reaktor omogućava brzo, gotovo trenutno miješanje reaktanata pomoću miješalice Kenics, vrlo kratko vrijeme reakcije od samo 15 s pri temperaturi od 155 °C, što u konačnici rezultira visokom produktivnošću od gotovo 1 kg h^{-1} produkta za reaktor volumena od 4,5 mL.

1.INTRODUCTION

Due to the very high demand for polyurethanes (with an annual production of over 5 million tons per year in Europe alone),[1] the manufacturing of polyisocyanates and their blocked counterparts is carried out at very large scale. Blocking reactions are typically very exothermic.[2] Slow addition of the blocking agent and careful control of the temperature of the reaction mixture during traditional batch processing is required, oftentimes limiting productivity.[3–5] A relevant example is the production of the blocked hexamethylene diisocyanate (HDI) trimer precursor B-HDIT, by reaction of the HDI trimer (HDIT) and methyl ethyl ketone oxime (MEKO) (Figure 1). HDIT is a commercially available trimer form of HDI, often selected for industrial applications owing to its reduced toxicity and volatility with respect to HDI, and especially its properties as a crosslinker for network formation in polyurethanes.[6] Preparation of B-HDIT is currently carried out in batches of over 10 tons scale. HDIT is added slowly, over a time-frame of several hours, to a stirred-tank-reactor containing MEKO. The final HDIT/MEKO proportion is carefully adjusted to fit the isocyanate content of the starting material in a 1:3 stoichiometry. Metal catalysts such as dibutyltin dilaurate or acetate are used as additives in some cases to ensure that the reaction reaches completion.[7–10]

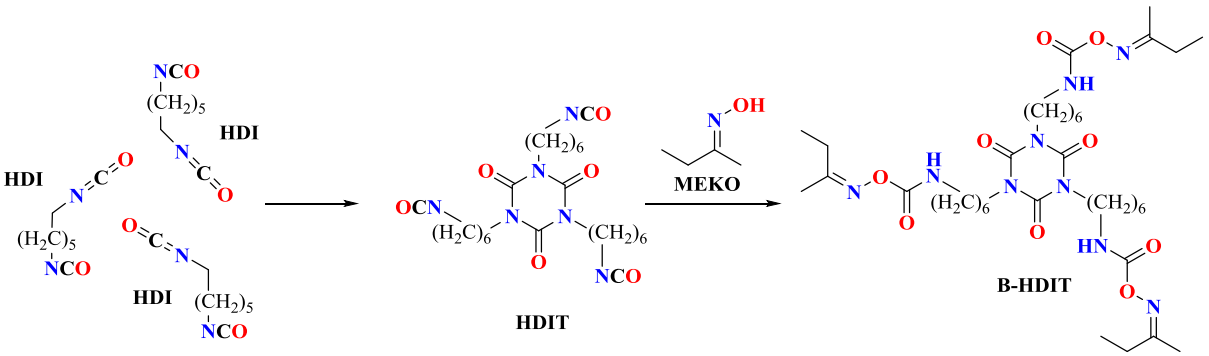

Figure 1. Preparation of HDIT from HDI as well as blocked B-HDIT from HDIT using MEKO.

An elegant manner to overcome the limitations of current batch procedures for the manufacturing of blocked isocyanates, and to ensure more robust processes and constant quality parameters, is to transfer the stirred-tank reactor protocols to continuous flow

procedures.[11–15] In a continuous flow reactor very efficient (essentially instantaneous) mixing can be achieved by implementing passive mixers (mixing geometry) to the reaction channel.[16–19] In addition, the high surface-to-volume ratio of continuous flow devices compared with batch reactors provides excellent heat- and mass-transfer to the system. Thus, exothermic transformations can be readily controlled with minimal risk of overheating or runaways. In this context, several examples of lab scale continuous flow procedures involving reactions between isocyanates and nucleophiles have been described in the literature.[20–23]

Notably, to the best of our knowledge, only one example of a continuous methodology for the preparation of blocked polyisocyanates can be found in the (patent) literature.[24] In the protocol developed by Cargill in the late 1970s, the reactants (polyisocyanate plus blocking agent) were fed with the desired stoichiometry into a reaction zone, from which the product was continuously withdrawn.[24]

The aim of this diploma work is to investigate the possibility of transferring the current batch procedure for preparing the B-HDIT into a continuous process starting from HDIT and MEKO. Initial batch optimization of the reaction will be conducted as well as testing the stability of the product at elevated temperatures by means of infrared (IR) spectroscopy as well as two-dimensional correlation infrared spectroscopy (2D-IRcorr), ^{1}H, and ^{13}C NMR spectroscopy and differential scanning calorimetry (DSC). The relatively high viscosity of HDIT (ca. 3000 mPa s at room temperature),[25] presents an additional issue for the translation of the batch process, which makes efficient mixing between the reactants troublesome, especially when large volumes are involved. For that reason the selection of a proper static mixer and reactor geometry is important; efficient mixing will be enabled by a Kenics® static mixer. Implementation of *in-line* Fourier transform infrared spectroscopy (FT-IR) analysis for the real-time monitoring of the continuous flow synthesis of a blocked isocyanate has not been reported. Furthermore, 2D-IR spectroscopy was used for the study of polymerization reactions,[26] and to the best of our knowledge, no such study was performed for the stability of blocked polyisocyanates.

2.LITERATURE REVIEW

In order to give a clear overview on the fields covered in this thesis, the literature review has been divided into three main sections. Starting with a flow chemistry section explaining the benefits of flow compared to the traditional batch processes followed by the chemistry of isocyanates and finally a section on IR spectroscopy for monitoring the progress of reaction concerning isocyanates and the possible decomposition process of the products at elevated temperature.

2.1. Flow Chemistry

Flow chemistry or continuous manufacturing has only fairly recently gained significant momentum in the pharmaceutical industry even though it was being largely used in the petrochemical and commodity chemicals industry. The small internal volume of flow reactors and their high surface area-to-volume ratios enhance mass and heat transfer, resulting in rapid mixing, and enabling precise control over the reaction parameters, increasing overall process efficiency. Furthermore, the small internal volume in microreactors translates to a minimal effective reaction volume at any given moment thus allowing the use of unstable or toxic intermediates or reagents in a safe manner. In addition, rapid exothermic reactions can safely be performed owing to the high mass- and heat-transfer rates.[11–15,27–29]

High heat transfer enables precise temperature control of the reaction by reducing the degree of side reactions thus outperforming the batch counterpart in view of selectivity (Figure 2). In cases where the reaction rate can be increased by increasing the reaction temperature, flow systems outperform their batch counterparts by enabling to safely go above the boiling point of the solvent, or by the ability to perform reactions with very short reaction times; even for so-called “runaway” reactions, where the heat of reaction increases the temperature of the medium, thereby increasing the rate of the reaction. This regime can lead to side-products or dangerous safety issues, such as rapid boiling of solvents, occasionally resulting in an explosion - can benefit from flow processes. An overall heat transfer coefficient (U) is commonly applied to the calculation of heat transfer in heat exchangers. In this application, U can be used to determine the heat transfer rate (q) where A_h is the heat transfer surface area and ΔT_{LM} is the logarithmic mean temperature difference (eq 1). By this

relationship, the rate of heat transfer is directly proportional to the surface area; thus, dissipation of heat is faster with larger surface areas. The advantage flow has over batch pertains to the reaction scale.

$$q = UA_h\Delta T_{LM} \quad \text{Eq. 1}$$

The resistance to heat transfer increases linearly with the size of the reactor channel. By simply prolonging the operation time, or scaling out, one produces more material.

The small dimensions of the flow reactor not only result in better heat transfer but also the better mixing, since mixing is often influential on the conversion and selectivity of reactions. Therefore, the degree to which mixing influences a reaction should be a major question when deciding whether or not to conduct an experiment in flow. Mixing describes the way two phases come together. Batch and flow reactors exhibit different mixing mechanisms which in combination with reaction kinetics will determine if flow conditions are beneficial. The Reynolds number (*Re*) is used to predict flow patterns in fluids, where ranges of *Re* divide mixing into three regimes: laminar, transitional, and turbulent. Low *Re* values correspond to laminar flow, whereas high *Re* values describe turbulent flow. Typically, mixing in laboratory-size batch reactors is laminar or transitional.[30] A transitional regime normally results in segregation inside the vessel, with turbulent mixing near the stir bar and laminar regimes at outlying parts. The movement of molecules to and from these isolated regions generally relies on diffusion.[31] Smaller vessels have smaller diffusion times; however, they are not capable of completely eliminating this segregation of mixing regimes. Tubular reactors inherently have much smaller diffusion times and achieve mixing much faster than in batch. Mixing, however, is more complicated than simple diffusion. The proper application of a mixer can better achieve homogeneity, and this reduces the amount of side-products. For certain reactions, flow reactors are used in fine chemical and pharmaceutical applications because high-intensity mixing can only be achieved using inline mixers.[30–32] Importantly, flow chemistry does not change the chemistry or kinetics of a reaction.[33] Rather, flow chemistry is a tool for chemists to eliminate or reduce concentration gradients that may be detrimental to extremely fast reactions. The rate of the reaction and mixing should be one of the major considerations when deciding whether or not to develop a flow process.

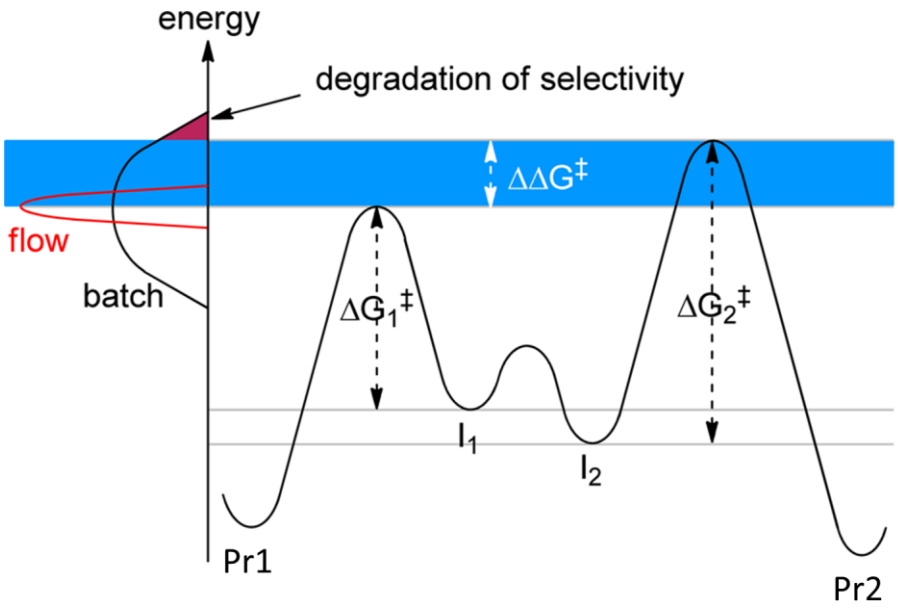

Figure 2. The narrow temperature profile of the reaction mixture in flow increases selectivity as compared to a wider temperature profile in a batch reactor. In this example, Pr_1 is the desired product and Pr_2 is a side-product. The blue area signifies the window for selective reactivity. Here, where a small difference in transition state energies ($\Delta\Delta G^{\ddagger}$) leads to unselective reactivity in batch due to the large temperature profile. Taken from: M. B. Plutschack, B. Pieber, K. Gilmore, P. H. Seeberger, *Chem. Rev.* **117** (2017) 11796–11893.

An additional advantage of flow reactors is the ease with which process analytical technology (PAT) tools can be integrated for reaction monitoring. Thus, continuous *in-line* UV-Vis, IR, and even NMR monitoring tools have been recently developed, enabling real-time measurements of reactants, products, or side-product concentrations in the reaction mixture stream.[34–36]

2.2. Isocyanate Chemistry

The isocyanate group is a highly reactive functional group which can be prepared by Curtius rearrangement,[37,38] it also appears as a non-isolable intermediate in Hoffman rearrangements[39–42] and in the Bucherer-Bergs reaction.[43] The Lossen rearrangement[44–46] affords isocyanates as one of the products together with the corresponding carboxylic acid (Figure 3). The Curtius rearrangement is a thermal or less often photochemical decomposition of an acyl azide to the corresponding isocyanate. The photochemical decomposition of an acyl azide is also known as Harger reaction.[47] The Curtius rearrangement can be applied to

carboxylic acids containing a wide range of functional groups, and isocyanates can be isolated if the reaction is conducted in the absence of nucleophile.

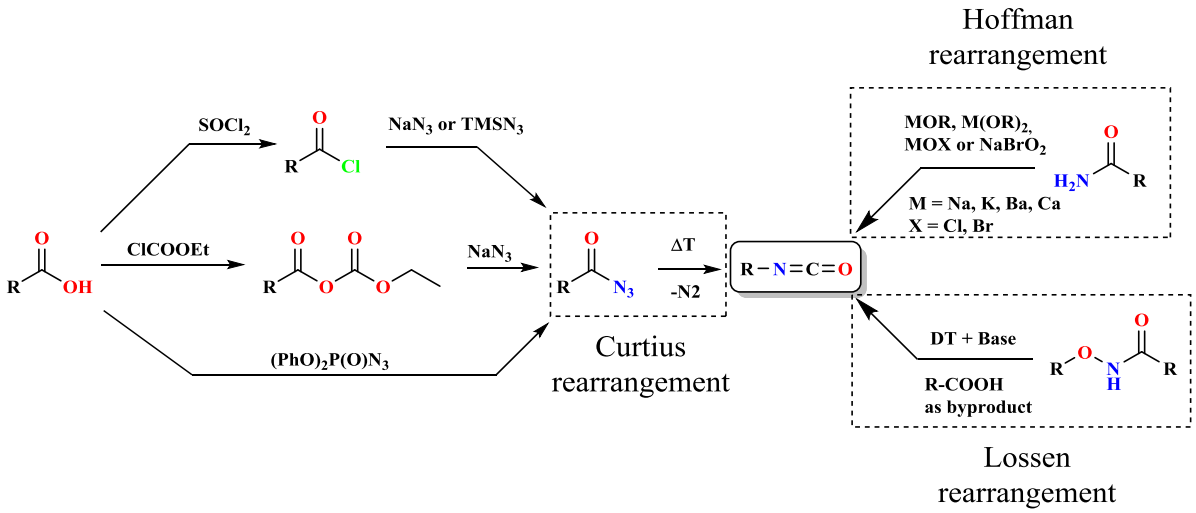

Figure 3. Reactions used to prepare isocyanate derivatives.

The two electronegative atoms oxygen and nitrogen respectively make the central carbon atom of the isocyanate highly electrophilic, thus making it susceptible to nucleophilic attack. For that reason, isocyanates are relatively reactive compounds and depending on the nature of the nucleophile provide a variety of useful compounds. If the nucleophile is water, the product of the reaction is an unstable carbamic acid, whereas if the nucleophile is alcohol being aromatic or aliphatic, the obtained product is an ester of carbamic acid. Equivalent to that if the nucleophile is nitrogen from an amine the products are amides of carbamic acid or better known as urea derivatives (Figure 4). [48,49]

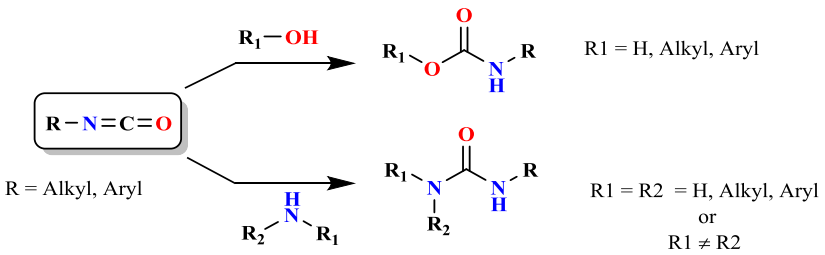

Figure 4. Reactions of the isocyanate group

Polyisocyanates are an important class of compounds in polyurethane chemistry, with a wide range of industrial applications such as the preparation of coatings, adhesives, foams, elastomers and isolating materials.[50–53] The isocyanate moiety, a key functional group for the

polymerization process, is reactive and toxic, which makes storage and utilization of these materials unpractical for many applications.[54] The handling of these substances is therefore generally problematical and strictly regulated. To overcome these drawbacks, the use of blocked isocyanates has been markedly increasing over the past few decades.[55] Blocked isocyanates are adducts formed by the reversible reaction of the isocyanate with a hydrogen-containing nucleophile, called "blocking agent" (Figure 5).[7–9] Typical blocking agents include phenol, MEKO, ε-caprolactam, imidazoles, or mercaptans. MEKO being the most common blocking reagent reported in the literature.[10] Blocked isocyanates are stable at room temperature - even in aqueous suspensions - providing urethane precursors with extended shelf-life that are easy-to-handle and safe due to their low toxicity.[7–10] The isocyanate can be regenerated at elevated temperatures in a process called de-blocking. This is typically carried out in the presence of the desired hydroxy-containing co-reactants to form the polyurethane during the curing process.[50] The deblocking conditions vary with the blocking agent utilized and can, therefore, be tailored for specific applications.[10]

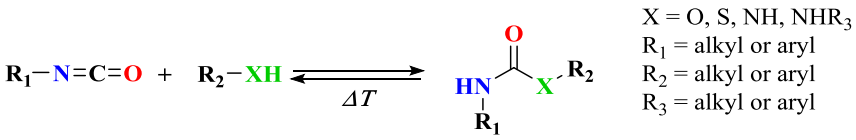

Figure 5. Blocking of the isocyanate.

Monitoring the progress of blocking/deblocking reactions of polyisocyanates in batch by means of chemical titration[56] and NMR spectroscopy[57,58] has been described. Thermogravimetric analysis (TGA) and differential scanning calorimetry (DSC) have also been utilized to evaluate deblocking temperatures.[59–61]

2.3. Infrared Spectroscopy

The study of interaction of electromagnetic radiation with a molecule is the subject of spectroscopy; the part of the electromagnetic spectrum falling into the range from 400 cm^{-1} to 4000 cm^{-1} and its interaction with the molecule is the subject of mid-infrared spectroscopy, refered to as IR spectroscopy. The energy of the mentioned part of electromagnetic radiation is sufficient to promote configurational changes of the molecule, vibrations being the fundamental configurational changes studied. When the wave of electromagnetic radiation passes through the sample it induces the vibrations of specific functional group, thus

attenuating the amplitude of the incoming wave. If the incoming wave frequency corresponds to the vibrational frequency of the functional group we say that the functional group absorbs the corresponding frequency. In IR spectroscopy, the frequency of the electromagnetic wave is not used directly, instead wavenumbers are used ($\tilde{\nu}$ in cm^{-1}). The fact that different functional groups in a molecule absorb at different wavenumbers is exploited to determine the presence of specific functional groups within the sample or study the dynamics of molecular interactions.[62,63]

FT-IR spectroscopy is the method of measuring the IR spectrum based on the interference of electromagnetic waves using a Michaelson interferometer and Fourier transformation. The advantage of using FT-IR as compared to a dispersive optics system is in the greater speed of the spectrum acquisition and since the instrument measures the whole spectrum (from 4000 cm^{-1} to 400 cm^{-1}) simultaneously it results in multiplex (or Felgett's) advantage. Additionally, the lack of an entrance slit for incoming light results in throughput (or Jacquinot) advantage making it superior in signal to noise ratio as well.[63]

2.3.1. One-dimensional Infrared Spectroscopy

For a molecule to absorb the IR radiation (i.e. to be IR active) it has to possess a specific feature: the dipole moment must change during the vibration. This so-called selection rule for IR spectroscopy is useful to describe and differentiate between IR active and IR inactive vibrations. IR spectra of molecules show a strong dependence on the environment of the molecule, permitting to study the interactions of the molecule within its environment. Typically if the molecules are associated as they are in the case of a liquid phase, the bands will be broader than in the gas phase. Amongst the molecular interactions in liquids the hydrogen bonding certainly plays an important role. In order to study the hydrogen bonding, arguably, the best technique is IR spectroscopy since the hydrogen bond lowers the force constant of the corresponding hydrogen bond donor (HBD), thus changing the frequency of absorbed radiation. That effect is most pronounced for OH stretching vibrations, whereupon for hydrogen bonding a shift of up to 1000 cm^{-1} can be observed for the center of an OH stretching vibration and it depends strongly on the strength of hydrogen bond. Other hydrogen bond donors, as well as hydrogen bond acceptors (HBA), are affected by hydrogen bonds. The amide functional group, possessing an HBD as well as HBA, is one of the more exploited functional groups to study hydrogen bonding.[64] The amide I band corresponding to the C=O

group stretching vibration experiences a negative shift (towards lower frequencies) upon hydrogen bonding in the range from –80 to –60 cm^{-1}. The amide II band originating from CNH bending usually found at 1510 cm^{-1} is shifted to higher wavenumbers by up to +50 cm^{-1}.[64]

The NCO group is a linear triatomic group consisting of nitrogen, carbon and oxygen. Because of different electronegativities for oxygen and nitrogen, the NCO group possesses a permanent dipole moment. Upon the absorption of IR radiation, the NCO group displays asymmetric vibration in the range from 2300 cm^{-1} to 2250 cm^{-1}, the intensity of which is usually very strong. Symmetric stretching of NCO is present in the region from 1460 cm^{-1} to 1340 cm^{-1} and is usually weak. Additionally, it displays Fermi resonance formally splitting the single o.ph.str. band to two bands of equal intensity.[62,63] By blocking the isocyanate with an oxime functionality NCO is transformed into a carbamic acid derivative (Figure 6). The band derived from the symmetric stretching of C=O (amide I) occurs in the region 1740 cm^{-1} to 1680 cm^{-1} and is highly susceptible to hydrogen bonding lowering its frequency. NH stretching occurs in the range from 3340 cm^{-1} to 3390 cm^{-1} if hydrogen bonding is present. The amide II band derived from a combination of NH bendning and N–C=O stretching is found in the region from 1530 cm^{-1} to 1500 cm^{-1}, whereas if hydrogen bonding is present the range is extended from 1600 cm^{-1} to 1500 cm^{-1} overlapping with NHC deformation found in the range from 1540 cm^{-1} to 1530 cm^{-1}. Finally, the oxime moiety possesses a strong OH vibration found in the 3300 cm^{-1} to 3130 cm^{-1} range, if hydrogen bonding is present, and in dilute solutions where there is no hydrogen bonding in the range from 3650 cm^{-1} to 2570 cm^{-1}. Imine (C=N) stretching is found in the range from 1690 cm^{-1} to 1640 cm^{-1} and finally a strong N–O vibration is found in the range from 1030 cm^{-1} to 870 cm^{-1}.[63–65]

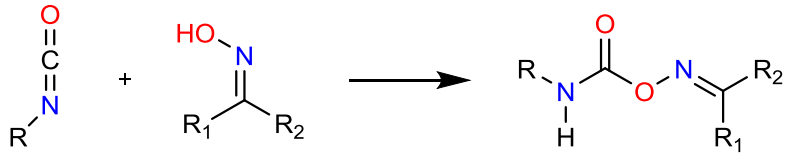

Figure 6. Blocking reaction of isocyanate and ketoxime producing the carbamic acid derivative.

FT-IR is often the method of choice to study the kinetics of blocking reactions or deblocking temperatures of polyisocyanates.[7–10] This is due to the characteristic and intense

band of the NCO group, which permits quantitative measurement of the NCO content in the mixture.[66] Such studies are typically carried out using attenuated total reflection (ATR) techniques, with the samples prepared as thin films with a thickness similar to that for the coating applications.[7–10]

2.3.2. Two-dimensional Infrared Spectroscopy

There are two different types of two-dimensional (2D) infrared spectroscopy (2D-IR) under the term two-dimensional infrared spectroscopy. One of which is coined as coherent two-dimensional infrared spectroscopy based on the breakthrough in ultrafast lasers. By employing ultrafast coherent laser pulses to form a pulse sequence, one can study the interactions of a specific functional group with another functional group, being either an intramolecular or intermolecular interaction on the picosecond time scale.[67] On the other hand, another type of two-dimensional spectroscopy called two-dimensional correlation spectroscopy (2Dcorr) is based on utilizing the external perturbation of the sample and measuring the one-dimensional (1D) spectra as the function of the perturbation. Thus, obtaining so-called dynamic spectra, by cross-correlation of 1D spectra one forms a 2Dcorr spectra.[68–74]

External perturbation can be mechanical, thermal, magnetic, chemical, acoustic or any type of stimulation inducing the change in the observed system. The response of the system to the perturbation leads to a superposition of spectral variations, producing the dynamic spectra. From the dynamic spectra and reference spectra using a Hilbert Noda transformation one obtains 2Dcorr spectra (Figure 7). It is worth pointing out that two-dimensional infrared correlation spectroscopy (2D-IRcorr) can be performed with any standard FT-IR spectrometer or dispersive type IR spectrometer simply by modifying the experimental setup in order to induce the change in the system and measuring 1D IR spectra while the system is changing.

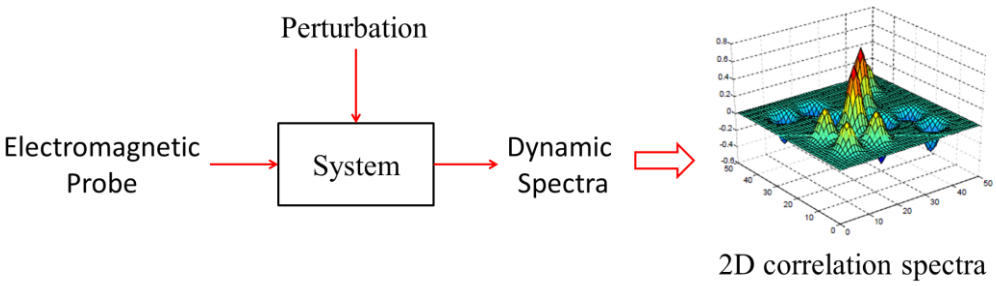

Figure 7. The principle of 2D correlation spectroscopy.

By applying the Hilbert Noda transformation to the set of dynamic spectra one obtains two orthogonal (real and imaginary) components known as synchronous and asynchronous 2D correlation intensities. Where synchronous represents an overall similarity or coincidental trend between two separate intensity variations measured at different spectral variables as the perturbation is scanned from minimal to maximal value. An asynchronous 2D correlation intensity may be thought as the measure of dissimilarity or out of phase spectral intensity variation.

A synchronous 2Dcorr spectrum is the symmetric spectrum with respect to the diagonal line corresponding to the coordinates (in 2D-IRcorr spectroscopy coordinates having the wavenumbers $\tilde{\nu}_1$ and $\tilde{\nu}_2$). Correlation peaks appear at both diagonal and off-diagonal positions. The intensity of peaks located at diagonal positions mathematically corresponds to the autocorrelation function of spectral intensity variations observed during an interval where perturbation varies from minimal to maximal value. It is worth mentioning that autopeaks are always positive. Representing the overall extent of spectral intensity variation observed at the specific spectral variable $\tilde{\nu}$ during the observation interval between minimum and maximum of perturbation. Thus, any region of a spectrum which changes intensity to a great extent under a given perturbation will show strong autopeaks, while those remaining near constant develop little or no autopeaks. In other words, an autopeak represents the overall susceptibility of the corresponding spectral region to change in spectral intensity as an external perturbation is applied to the system. Cross peaks located at the off-diagonal positions of a synchronous 2D spectrum represent simultaneous or coincidental changes of spectral intensities observed at two different spectral variables $\tilde{\nu}_1$ and $\tilde{\nu}_2$. Such a synchronized change, in turn, suggests the possible existence of a coupled or related origin of the spectral intensity variations. It is often useful to construct a correlation square joining the pair of cross peaks located at opposite sides of a diagonal line drawn through the corresponding autopeaks to show the existence of coherent variation of spectral intensities at these spectral variables. While the sign of autopeaks is always positive, the sign of cross peaks can be either positive or negative. The sign of a synchronous cross peak becomes positive if the spectral intensities at the two spectral variables corresponding to the coordinates of the cross peak are either increasing or decreasing together as functions of the external variable during the observation interval. On the other hand, a negative sign of the cross peak intensity indicates that one of the spectral intensities is increasing while the other is decreasing (Figure 8).

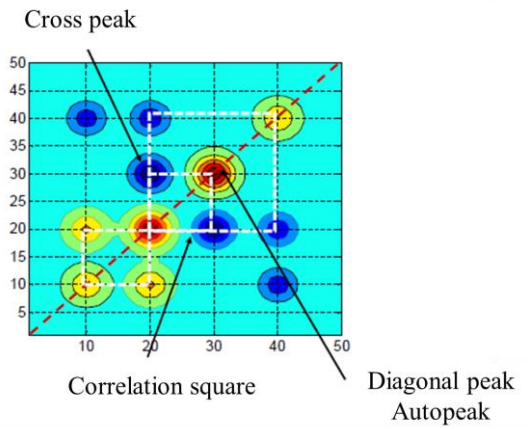

Figure 8. An example of synchronous 2D-IRcorr spectra. Taken and modified from P. D. B. Hannington, A. Urbas, P. J. Tandler, *Chemom. Intell. Lab. Syst.* **50** (2000) 149–174.

The intensity of an asynchronous spectrum represents sequential or successive, but not coincidental, changes of spectral intensities measured separately at $\tilde{\nu}_1$ and $\tilde{\nu}_2$. Unlike a synchronous spectrum, an asynchronous spectrum is antisymmetric with respect to the diagonal line. The asynchronous spectrum has no autopeaks, and consists exclusively of cross peaks located at off-diagonal positions. By extending lines from the spectral coordinates of cross peaks to the corresponding diagonal positions, one can construct asynchronous correlation squares. An asynchronous cross peak develops only if the intensities of two spectral features change out of phase with each other. For example, chemical functional groups experiencing different effects from some external field. Even if spectral bands are located close to each other, as long as the characteristic patterns of sequential variations of spectral intensities along the external variable are substantially different, asynchronous cross peaks will develop between their spectral coordinates. As in the case of synchronous spectra, the sign of an asynchronous cross peak can be either negative or positive. It provides useful information on the sequential order of events observed. The sign of an asynchronous cross peak becomes positive if the intensity change at $\tilde{\nu}_1$ occurs predominantly before that at $\tilde{\nu}_2$ in the sequential order. On the other hand, the peak sign becomes negative if the change at $\tilde{\nu}_1$ occurs predominantly after $\tilde{\nu}_2$. However, this sign rule is reversed if the synchronous correlation intensity at the same coordinate becomes negative (Figure 9).

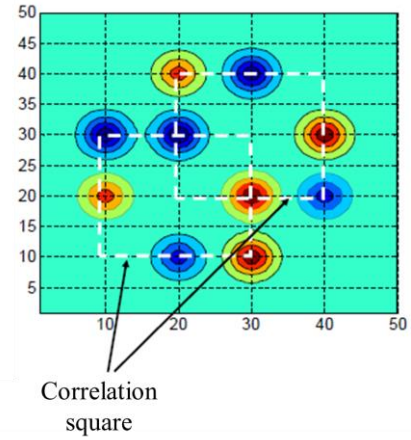

Figure 9. An example of asynchronous spectra. Taken and modified from P. D. B. Hannington, A. Urbas, P. J. Tandler, *Chemom. Intell. Lab. Syst.* **50** (2000) 149–174.

The basic interpretation of 2D-IRcorr spectra is simplified by a couple of rules known as Noda rules based on simulation studies. In the case of two overlapping bands changing their intensity separately, where one band increases in intensity, and other decreases, the characteristic four-leaf clover pattern emerges in synchronous spectra, while asynchronous show two well resolved cross peaks without any other features (Figure 10).

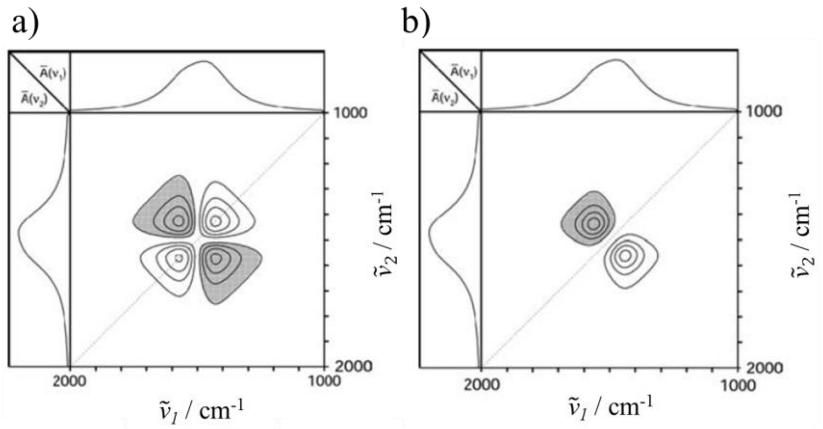

Figure 10. Synchronous (a) and asynchronous (b) spectra in the case of two overlapping bands changing intensity separately. Taken from I. Noda, Y. Ozaki, *Two-dimensional Correlation Spectroscopy – Applications in Vibrational and Optical Spectroscopy,* John Wiley & Sons, Chichester, 2004, pp. 57–64.

In case of one band position shift, the pattern in synchronous spectra again resembles a four-leaf clover with correlation peaks located closer to the diagonal. While it is difficult to

resolve those two cases on the basis of the synchronous spectra, in the asynchronous spectra a characteristic pattern resembling a butterfly emerges (Figure 11).

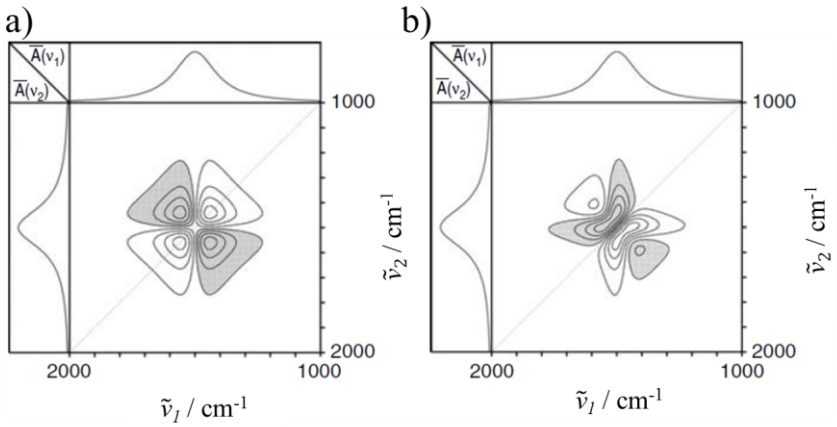

Figure 11. Synchronous (a) and asynchronous (b) spectra in the case of one band position shift. Taken from I. Noda, Y. Ozaki, *Two-dimensional Correlation Spectroscopy – Applications in Vibrational and Optical Spectroscopy*, John Wiley & Sons, Chichester, 2004, pp. 57–64.

In case of one band position shift coupled with an intensity change the patterns that emerge are: the distorted or disproportional four leaf clover resembling "angel" in synchronous spectra, and the distorted butterfly pattern in asynchronous spectra (Figure 12).

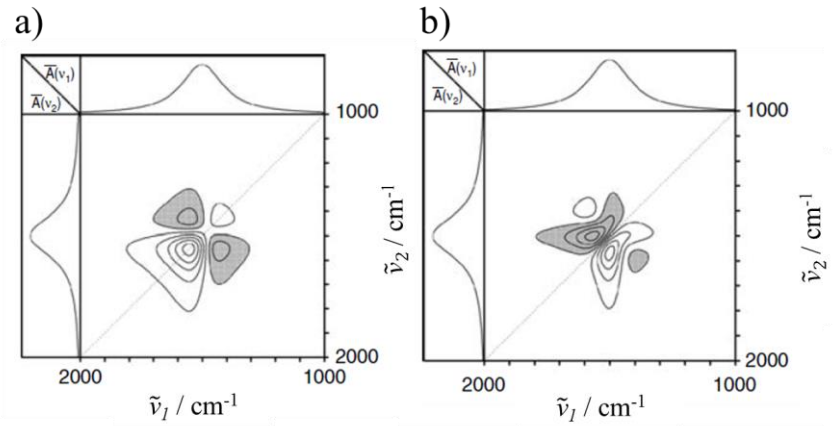

Figure 12. Synchronous (a) and asynchronous (b) spectra in the case of one band position shift coupled with intensity change. Taken from I. Noda, Y. Ozaki, *Two-dimensional Correlation Spectroscopy – Applications in Vibrational and Optical Spectroscopy*, John Wiley & Sons, Chichester, 2004, pp. 57–64.

Finally, in the case of line broadening, there is a characteristic four-way symmetric pattern consisting of a dominant central autopeak with a minor surrounding autopeak and negative cross peaks in the synchronous spectra. In the asynchronous spectra a fouraway symmetric cross resembling pattern is visible (Figure 13).

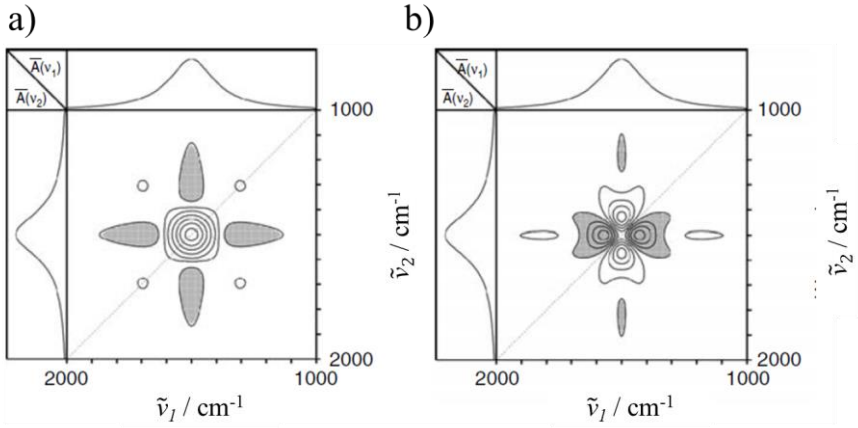

Figure 13. Synchronous (a) and asynchronous (b) spectra in the case of line broadening. Taken from I. Noda, Y. Ozaki, *Two-dimensional Correlation Spectroscopy – Applications in Vibrational and Optical Spectroscopy*, John Wiley & Sons, Chichester, 2004, pp. 57–64.

One of the first reports om using 2D-IRcorr spectroscopy was to study the evaporation of methyl ethyl ketone/toluene solvent mixture for dissolving polystyrene.[75] Furthermore, 2D-IRcorr spectroscopy was used to examine hydrogen bonding and dissociation of basic molecules like N-methyl acetamide,[76,77] transitions of oleic acid[78,79] and the reorientation of nematic liquid crystals induced by an electric field.[80] In the polymer field, one of the first studies was conducted on temperature and pressure effects on polyethylene[81] followed by extensive studies on various other polymers and liquid crystals.[82–85] To the best of our knowledge, the only report in the literature on the study of isocyanate-based polymers and their stability by correlation spectroscopy is on a 4,4'-diphenylmethane diisocyanate/1,4-butanediol thermoplastic. Multiple exotherms and intermolecular interactions were studied by moving-window two-dimensional correlation infrared spectroscopy.[86]

3. EXPERIMENTAL SECTION

In the experimental section, a detailed description of the conducted experiments will be provided. The experimental section is divided into several parts concerning general information about used equipment and chemicals, followed by an analytical part for the stability of synthesized compounds and analysis of reactions and finally with the synthesis of compounds in batch as well as in a continuous manner.

3.1. General Remarks

^{1}H NMR spectra were recorded on a Bruker 300 MHz instrument. ^{13}C NMR spectra were recorded on the same instrument at 75 MHz. Chemical shifts (δ) are expressed in ppm downfield from TMS as an internal standard. The letters s, d, t, q, and m are used to indicate singlet, doublet, triplet, quadruplet, and multiplet. FT-IR analysis was performed using a Mettler Toledo ReactIR 15 spectrometer equipped with a silicon probe, and a resistive temperature detector (RTD) calibrated by two-point calibration using water ice mixture at 0 °C and boiling water at 100 °C. Commercially available hexamethylene diisocyanate trimer, HDIT (Desmodur N3300, Covestro, Lot # 0100084830, 21% NCO content) and methyl ethyl ketoxime, MEKO (Additol XL 297 – INT, Allnex Lot # WD0110985) were utilized. Solvent n-butyl acetate (99+ % purity) was purchased from Alfa Aesar and used without further purification.

3.2. Determination of Limit of Detection and Limit of Quantification

A series of solutions of HDIT in n-butyl acetate of 15, 14, 12, 10 and 8 mmol L^{-1} concentration were prepared and analyzed by FT-IR spectroscopy using a Mettler Toledo ReactIR 15. Five spectra were recorded for each sample with an average of 265 scans per spectra. Absorbance values of the band at 2216 cm^{-1} were extracted and used for calculating the average, standard deviation, limit of detection (LOD) and limit of quantification (LOQ) (Figure 22).

3.3. Differential Scanning Calorimetry

The DSC analyses were carried out using a 204 F1 Phoenix instrument (Netzsch). Samples of ca. 5 mg were placed in an aluminum pan with the lid pierced. A heating ramp of 5 °C min^{-1}

was applied to up to 250 °C, using an empty pan as a reference. Nitrogen was used as an inert gas with a flow rate of 50 mL min^{-1}.

3.4. Temperature Stability Evaluation

The evaluation of temperature stability of B-HDIT was conducted using a dry 25 mL round bottom flask loaded with 8 g of B-HDIT and a magnetic stir bar. The IR probe was placed vertically over the sample and immersed ca. 3 mm in the mixture. The sample was heated at the desired temperature under stirring using a standard hot plate equipped with an internal temperature probe. Heating was adjusted so that the ramp of 8 °C min^{-1} was achieved until the sample reached the desired temperature of 160 °C. The IR spectra were collected in intervals of 15 s (an average of 125 scans per spectrum). The second part of the stability test was conducted in a manner that a sample of B-HDIT was heated at 180 °C for 1 h under stirring using a standard hot plate equipped with an internal temperature probe and the IR probe immersed in the sample (ca. 3 mm deep). The IR spectra were collected in intervals of 1 min (an average of 265 scans per spectrum). For the temperature ramps of stability test see Figure 14.

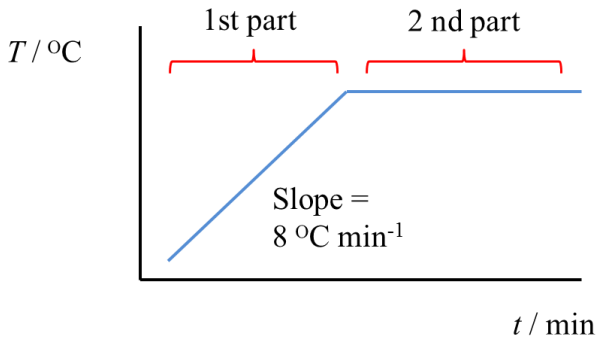

Figure 14. Two parts of investigated thermal stability of B-HDIT followed by FT-IR and 2D-IRcorr spectroscopy.

3.5. Preliminary Batch Experiments

15 mmol of HDIT (7.5 g) was placed in a 50 mL three-necked round-bottomed flask. A mechanical mixer was immersed in the liquid material using the vertical neck of the flask. The FT-IR probe was introduced into the liquid using a side neck of the flask, with an angle of 25° with respect to the mechanical stirrer. The starting material was preheated under stirring at the desired temperature (see Figure 15). Dibutyltin dilaurate (1 mol %) was added if needed. When the substrate reached the desired temperature, MEKO (40 mmol, 3.5 g) was

added with a syringe as fast as possible under vigorous stirring. Temperature and IR spectra were recorded in intervals of 15 s.

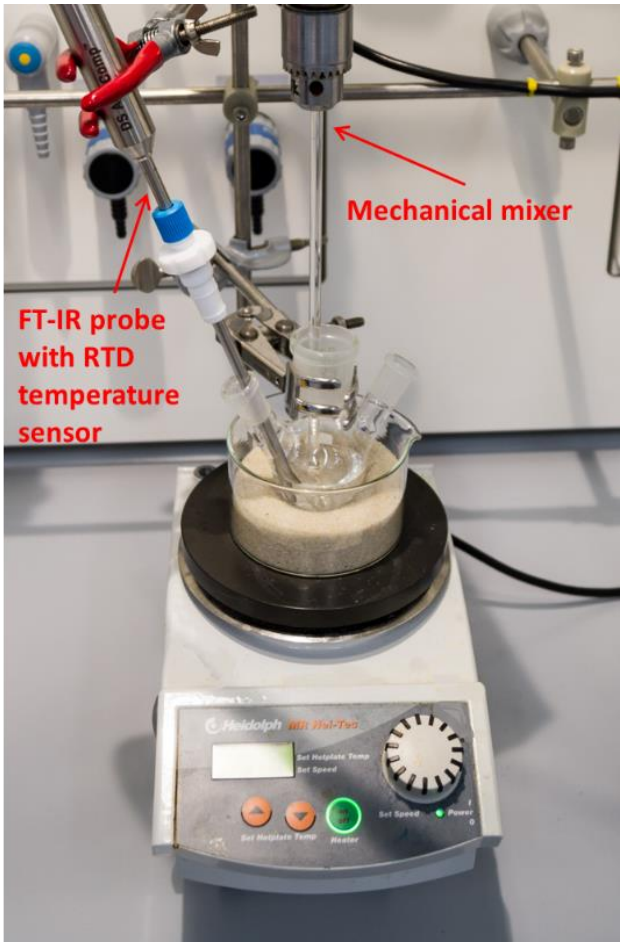

Figure 15. The setup used for the preliminary batch experiments.

3.6. Continuous Flow Synthesis of B-HDIT

The continuous flow reactor depicted in Figure 16 was utilized. The setup consisted of two reactant streams containing neat HDIT and MEKO. HDIT was pumped using a Vapourtec SF10 pump equipped with a viscous solvents kit. MEKO was pumped using a syringe pump (Syrris Asia). The two streams were mixed using a modified Y-connector in which MEKO is injected to the center of the HDIT stream. The mixture then entered a mixing unit, consisting of 3.2 mm i.d. perfluoroalkoxy (PFA) tubing containing 3 mm o.d. polypropylene Kenics® static mixers (0.98 mL dead volume, 12.5 mm length). The homogeneous mixture obtained

after the mixing unit entered a jacketed residence time unit, constructed in the manner of a tube in tube system with the inner residence time tube being perfluoroalkoxy (PFA) tubing, 3.2 mm internal diameter (i.d.), 4.8 mm outer diameter (o.d.) and the outer tube a high temperature silicone tube (15 mm i.d.) The thermal fluid was high temperature silicone oil (SilOil P20.275.50) temperature of which was controlled using Huber thermostat (CC304). *In-line* FT-IR analysis was implemented by incorporating a T-connector at the reactor outlet, to which the FT-IR probe was installed. The liquid stream and the IR probe were installed in a linear fashion so that the liquid stream turned 90° in the T-connector (Figure 17).

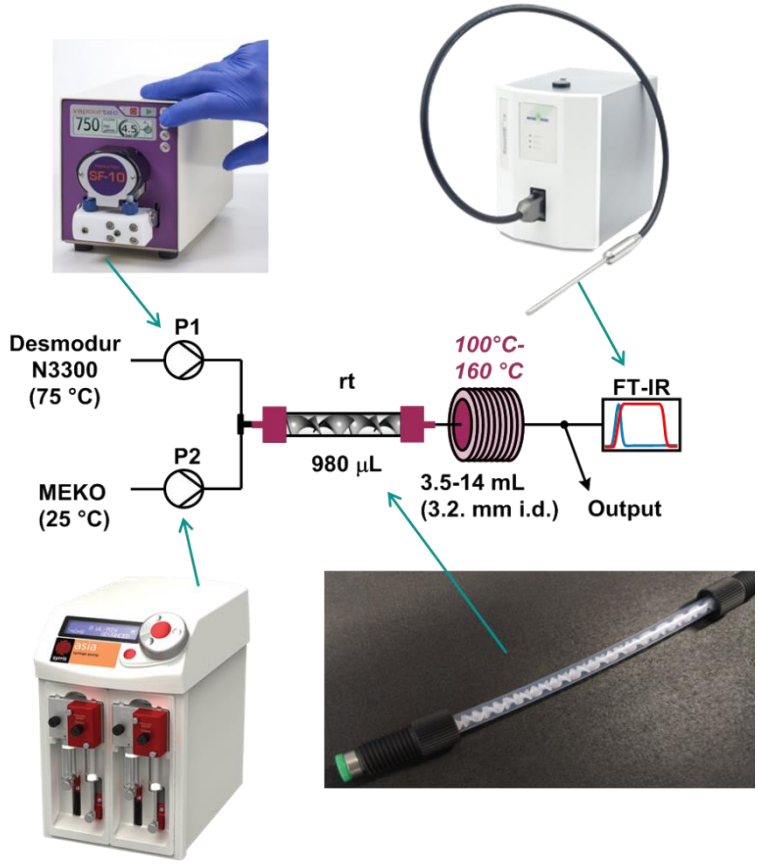

Figure 16. The schematic depiction of continuous flow reactor with pictures of used pumps Mettler Toledo ReactIR and constructed Kenics type static mixer.

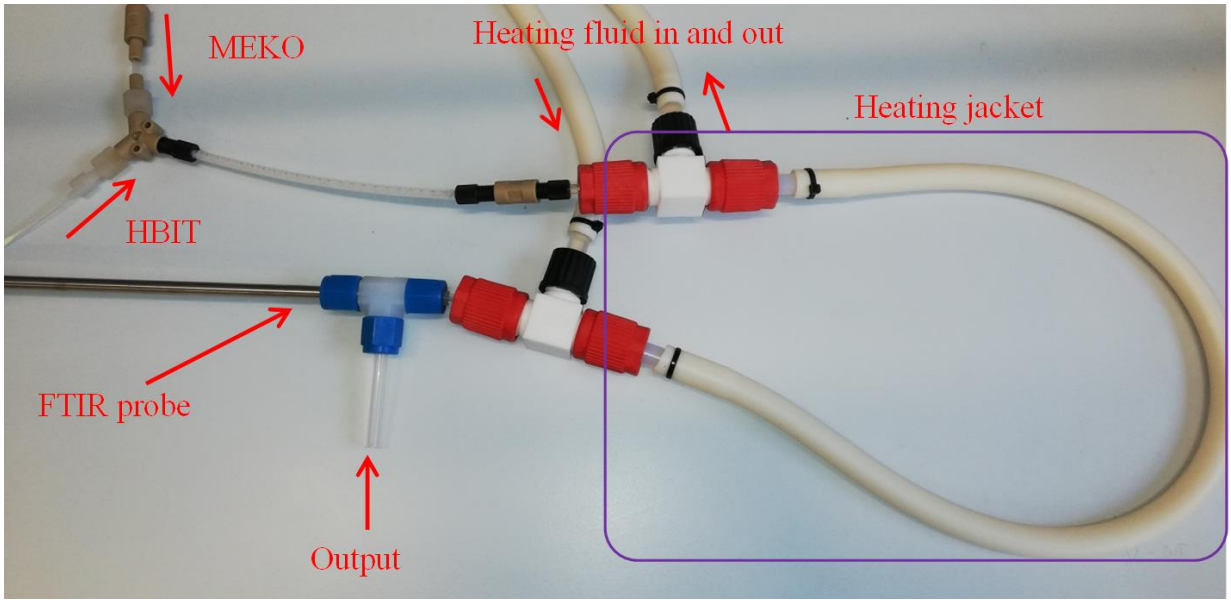

Figure 17. Picture of the designed reactor.

3.6.1. Continuous Synthesis of B-HDIT. Preparative Experiment under Intensified Conditions

Using the setup and method described above, a residence time unit of 3.5 mL was installed, and its temperature adjusted to 155 °C. The flow rates of the HDIT and MEKO feeds were set to 8.7 mL min^{-1} and 5.4 mL min^{-1}, respectively. Once the system was stable (monitored by inline FT-IR analysis) the neat, pure product was collected from the reactor output for 3.5 h (3.3 kg, quantitative yield).

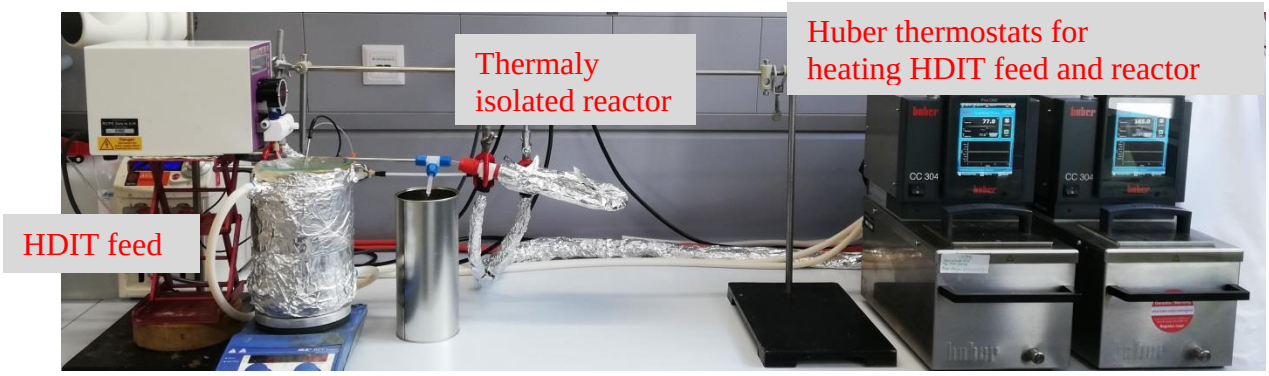

Figure 18. Picture of the system for the 3.5 h run.

1,3,5-Tris[6-[[[[(1-methylpropylidene)amino]oxy]carbonyl]amino]hexyl]-1,3,5-triazine-2,4,6(1H,3H,5H)-trione (B-HDIT). Obtained as a mixture of *E*/*Z* isomers (9 possible combinations) at the oxime position, with an average *E*/*Z* ratio of 2:5; *E* isomer: ^{1}H NMR ($CDCl_3$, 300 MHz) δ 6.32 (s, 1H), 3.81 (t, J = 7.8 Hz, 2H), 3.22 (q, J = 6.9 Hz, 2H), 2.42 (q, J = 7.8 Hz, 2H), 1.92 (s, 3H), 1.59–1.50 (m, 4H), 1.34–1.31 (m, 4H), 1.06 (t, J = 7.5 Hz, 3H); *Z* isomer: ^{1}H NMR ($CDCl_3$, 300 MHz) δ 6.32 (s, 1H), 3.81 (t, J = 7.8 Hz, 2H), 3.22 (q, J = 6.9 Hz, 2H), 2.26 (q, J = 7.5 Hz, 2H), 1.96 (s, 3H), 1.59–1.50 (m, 4H), 1.34–1.31 (m, 4H), 1.09 (t, J = 7.5 Hz, 3H).

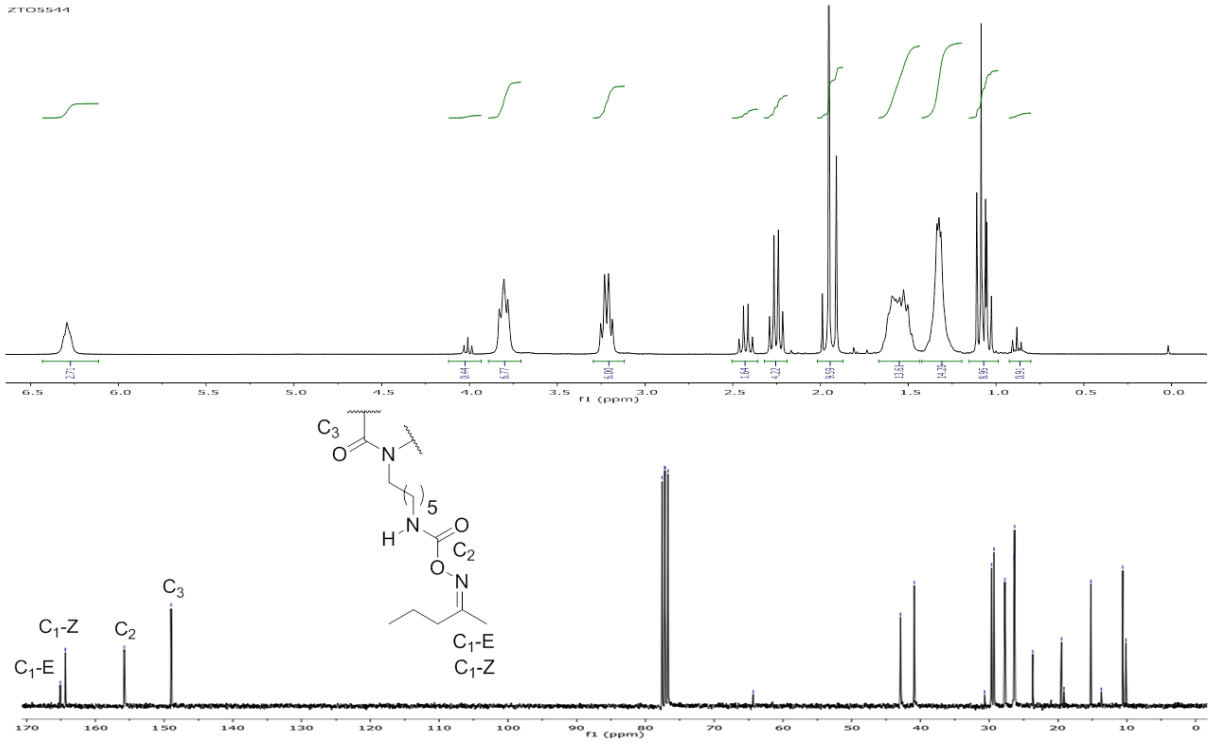

Figure 19. ^{1}H and ^{13}C NMR spectra of the product B-HDIT directly obtained from the output of the continuous flow reactor at 155 °C (15 s residence time).

4. RESULTS AND DISCUSSION

4.1. FT-IR Analysis: Assignment, Signal Calibration, Limitations, and *in-line* implementation

FT-IR spectroscopy is a well-known analytical tool for monitoring blocking/deblocking reactions of isocyanates.[7–10] A Mettler Toledo ReactIR 15 spectrometer, equipped with a silicone probe was utilized in all experiments described herein. This probe permits simultaneous FT-IR measurement and temperature monitoring. The isocyanate group typically absorbs in the range of 2300–2200 cm^{-1}. Analysis of a neat sample of HDIT and B-HDIT (Figure 20) revealed two overlapping bands at 2297 cm^{-1} and 2230 cm^{-1} for the NCO group in the HDIT sample (Figure S1), most likely due to Fermi resonance.[87,88] As expected, these bands fully disappear for the MEKO blocked product B-HDIT (0 % NCO content), while a band at 1725 cm^{-1} corresponding to the carbamate carbonyl stretching can be observed. The bands at 1502 cm^{-1} and 1205 cm^{-1} can be observed for B-HDIT coming from CNH out of phase bending (o.ph.bend) and the in-phase bending (i.ph.bend), respectively, as expected these two bands are not present in HDIT spectra. In both spectra, C_1=O stretching vibration at 1685 cm^{-1} coming from urea (carbonyl groups on the ring) is found together with the band at 1331 cm^{-1} coming from NCN o.ph.bend, later being of higher intensity in HDIT than is found in B-HDIT. Vibrations from methylene groups are found in both spectra at 1458 cm^{-1}, 1376 cm^{-1} and 764 cm^{-1} coming from CH_2 bending, N_1–CH_2 bending and CH_2 in phase rocking (i.ph.rock), respectively. The B-HDIT has new vibration appearing at 1357 cm^{-1} coming from methyl groups in phase bending (i.ph.bend). Strong N–O vibration appearing at 894 cm^{-1} is present in B-HDIT as well as weak C=N vibration appearing as a shoulder at 1652 cm^{-1} (presence of C=N vibration is significantly pronounced in synchronous 2D-IRcorr spectra) additionally confirming the presence of oxime moiety in B-HDIT (see Table 1, and Figure S2 in Appendix for zoomed in view of the 1800–1100 cm^{-1} spectral range).

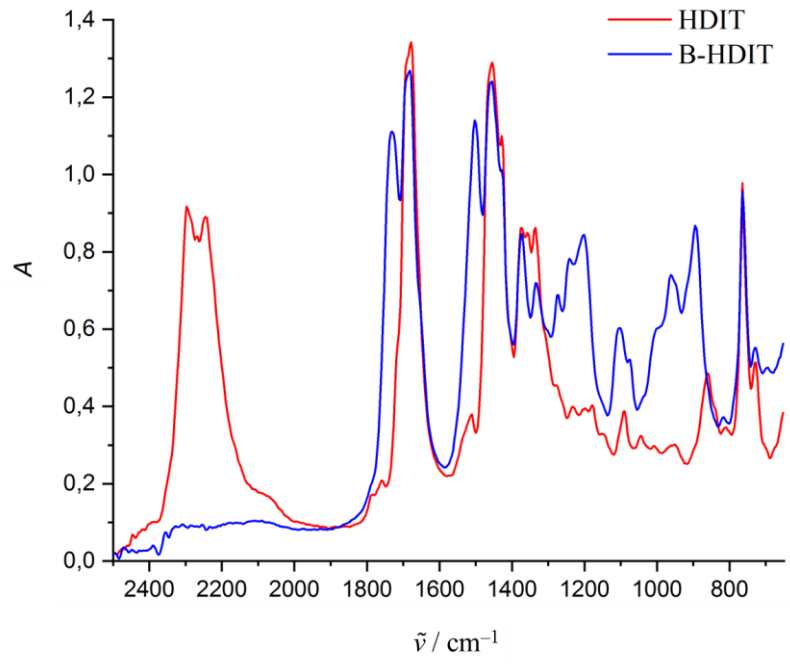

Figure 20. FT-IR spectra of neat polyisocyanate HDIT and MEKO-blocked B-HDIT.

Table 1. The assignment of selected vibrations in FT-IR spectra of HDIT and B-HDIT samples together with part of the structure for respective molecules.

Vibration / cm^{-1}	B-HDIT	HDIT
2297		
2233		NCO (Fermi resonance)
1725	C2=O stretch	
1685	C1=O stretch	C1=O stretch
1502	C-N-H o.ph.str	
1458	-CH2- bend	
1428		-CH2-NCO bend
1376	-CH2-NCO bend	
1331	N-C-N o.ph.bend	
1205	C-N-H i.ph.str	
894	N-O bend	
764	CH2- i.ph.bend	

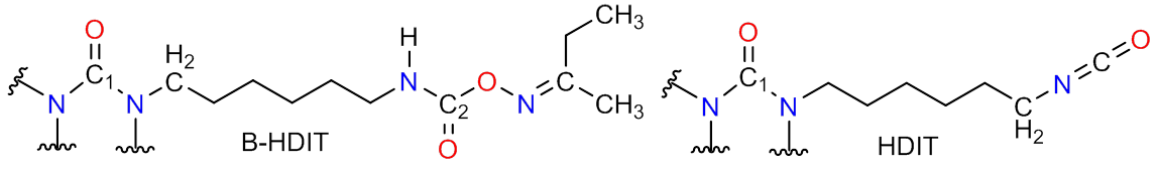

Calibration of the IR spectrometer for quantitative analysis was carried out by analyzing a series of samples containing mixtures of pure HDIT and B-HDIT. By carefully adjusting the amount of both components different blocking reaction conversions (in terms of % NCO) were simulated. Due to the very high concentration (neat) of the samples and the high sensitivity of the spectrometer, the IR signal was saturated for pure HDIT and only started to decrease for mixtures with a composition below 50 % HDIT (Figure 21). Linearity between the IR signal and the isocyanate concentration suitable for quantification was only observed for mixtures with an HDIT concentration below 30 % (Figure S3). Thus, during a blocking reaction, conversions in the range of 70–100 % could be quantified. Although the high sensitivity of the spectrometer allowed for detection of small quantities of NCO, data at the initial stages of the reaction (conversions below 70 %) could not be obtained. Consequently, the analytical method was suitable for early stages of the reverse deblocking process, but could not be used for quantifying progress of deblocking reactions above 30 % conversion.

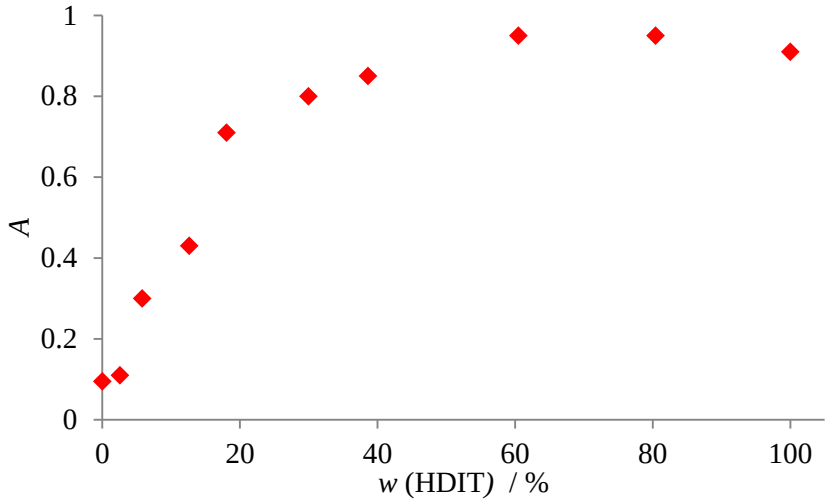

Figure 21. The intensity of the NCO absorption band at 2261 cm^{-1} as the function of the content of HDIT in a mixture with its MEKO-blocked counterpart B-HDIT.

To determine the LOD and LOQ of the FT-IR spectrometer for NCO in a mixture, a series of solutions of known concentration of HDIT in n-butyl acetate were prepared. A non-viscous solvent was utilized in this case to facilitate accurate preparation of very diluted solutions, ranging from 8 mmol L^{-1} to 15 mmol L^{-1} (Figures 22a and 22b). Using the equation $S_m = S_{bl} + k\sigma_{bl}$ and taking the constant k = 3 for the calculation of the LOD and k = 5 for the

LOQ, where S_m presents the minimal analyticaly distinguishable signal for LOD and LOQ respectively. The standard deviation for the blank sample (σ_{bl}) was calculated to be 0.004 07 at 2261 cm^{-1}, while the signal for the blank sample (S_{bl}) was calculated to be 0.009 48. This corresponds to a LOD of 7 mmol L^{-1} and an LOQ of 9.7 mmol L^{-1}.

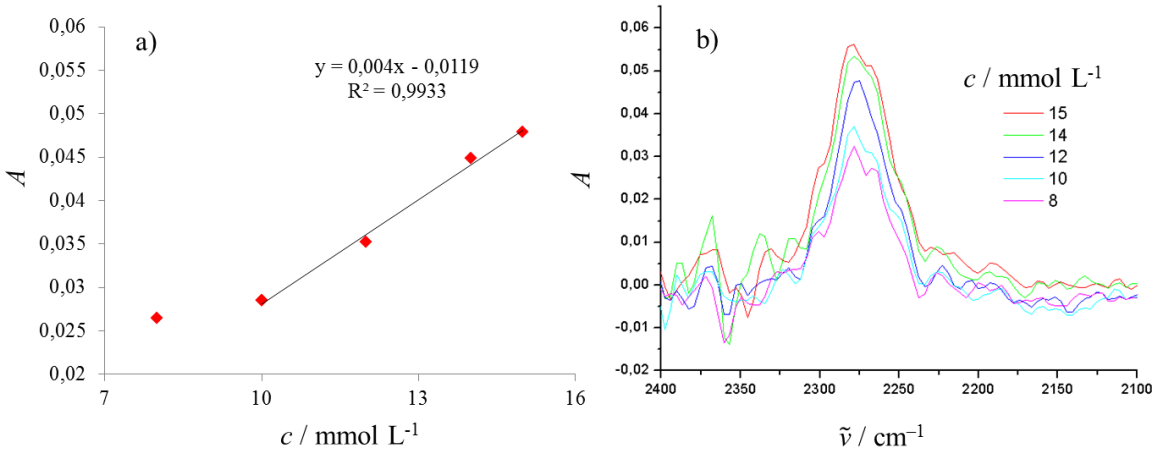

Figure 22. a) Calibration diagram depicting the LOD at 7 mmol L^{-1} and a linear range of quantification starting at 9.7 mmol L^{-1} (LOQ) and b) FT-IR spectra of diluted solutions of HDIT in n-butyl acetate.

4.2. Thermal Stability of B-HDIT

Deblocking of MEKO-blocked isocyanates typically takes place at temperatures above 120 °C.[7–10] Methods to evaluate deblocking temperatures include FT-IR, TGA and DSC analysis. In these experiments, it is important that the sample is prepared in a manner that MEKO can evaporate.[89,90] FT-IR, for example, is usually carried out applying a thin layer of the blocked compound, which facilitates evaporation of the blocking agent as well as recovery and detection of the isocyanate.[7–10,89] This is similar to the curing processes, that can lead to undesired bubbles in the polymer if the blocking agent is not able to evaporate. The high viscosity of both HDIT and B-HDIT could in principle obstruct evaporation of MEKO from an overheated reaction mixture. This, in addition to the lack of headspace in a continuous flow reactor, could enable the synthesis of B-HDIT in the range of its deblocking temperature without loss of MEKO during the process. With this in mind, we evaluated the thermal stability of B-HDIT by DSC, FT-IR and NMR analysis.

4.2.1. DSC Analysis

DSC analysis of B-HDIT revealed a broad, slight endotherm starting at ca. 170–175 °C up to 220 °C, which could correspond to the deblocking reaction (Figure 23). Such broad signals have been previously described for isocyanate deblocking in some cases.[91] At elevated temperatures (> 220 °C) a slightly exothermic event (< 1 mW mg^{-1}) could be detected, which likely corresponds to product degradation.

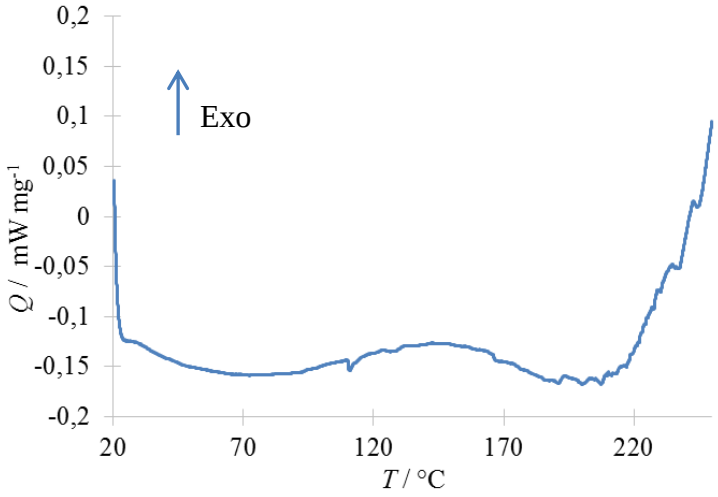

Figure 23. DSC analysis of B-HDIT.

4.2.2. B-HDIT Temperature Stability Study using IR and NMR Spectroscopy

Variable temperature FT-IR monitoring experiments were carried out in a 25 mL round bottom flask, in which 15 mmol of B-HDIT and a stir bar were placed. The IR probe was placed vertically, and immersed approximately 3 mm into the viscous liquid. Heating was initiated at the speed of 8 °C min^{-1} from room temperature to 160 °C. During the heating IR spectra were recorded in intervals of 15 s and data were processed using 2Dshige software.[92] Analysis of all the correlations in the 2D-IRcorr spectra (Figure S4 and S5) would be beyond the scope so we have limited ourselves to the carbonyl group of the carbamate and urea being the functional groups of interest. Synchronous correlation spectra are shown in the region from 1800 cm^{-1} to 1400 cm^{-1}. Apart from higher resolution of vibrations in 2D-IRcorr spectra (as can be seen from the well resolved C=N vibration) the high intensity autocorrelation for the C_1=O, C_2=O, C=N as well as CH_2 is noteworthy, indicating the high degree of change for the respective functional groups during the heating process (Figure 24). Most prominent is the appearance of two “angel-like” clusters of correlation peaks. A read correlation square indicates the shift towards higher frequencies for the C_2=O group, the reason for it being the

breaking of the hydrogen bonds formed between the respective carbonyl group and hydrogen bond donor (most likely the NH from the carbamate), since the very opposite happens upon formation of a hydrogen bond with a carbonyl group.[64] The black correlation square indicates the shift of the center of the C=N vibration toward higher frequencies again in agreement with the breaking of the hydrogen bond. The formation of a hydrogen bond with C=N tends to shift the center of the vibration band toward lower wavenumbers.[93] Correlation of C_2=O and C=N group respectively with CNH o.ph.str. is visible (dashed red for C_2=O and black correlation square for C=N group). In addition, the asynchronous spectra support the correlations from the synchronous spectra with the two overlapping butterfly-like patterns, and correlation of CNH with C_2=O and C=N again noted with dashed red and black correlation squares for respective groups (Figure 25). It can be concluded that upon heating of the sample only the hydrogen bonds between the hydrogen bond donor groups and the hydrogen bond acceptor groups are being broken and no formal covalent bond breaking occurs, indicating the stability of the product. Lastly, the sample was heated at 180 °C for 1 h, while IR spectra were recorded with intervals of 1 min. Notably, no signal corresponding to the isocyanate group could be observed (Figure S5).

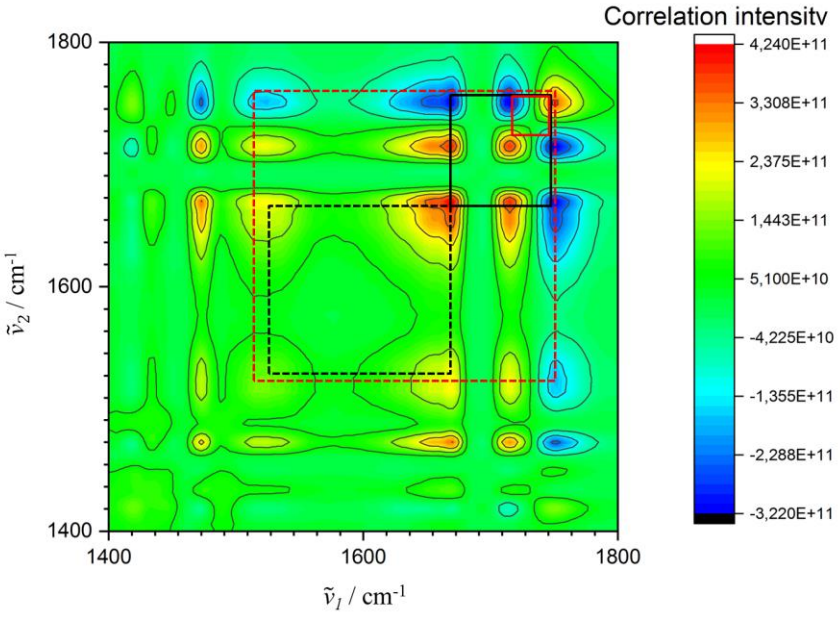

Figure 24. The synchronous 2D-IRcorr spectra of B-HDIT during heating from room temperature to 160 °C in the region from 1400 cm^{-1} to 1800 cm^{-1}.

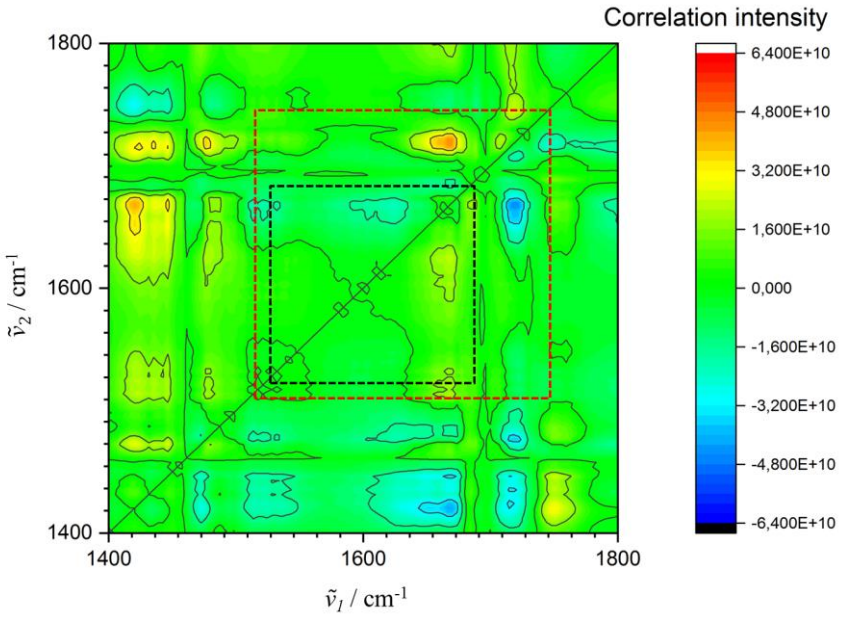

Figure 25. The asynchronous 2D-IRcorr spectra of B-HDIT during heating from room temperature to 160 °C in the region from 1400 cm^{-1} to 1800 cm^{-1}.

Likewise, in 2D-IRcorr spectra, there is no indication for an isocyanate group appearance (Figure 26). The only correlation is between C_1=O, C_2=O, C=N and CNH groups similar to the previous 2D-IRcorr experiment but with much smaller correlation intensity (around 11 orders of magnitude smaller, see correlation intensity at Figure 24 and 25). Such small correlation intensity is not significantly above the noise of the instrument so no correlation can be deduced from data, indicating the absence of any detectable change with functional groups of interest upon heating for 1 h at 180 °C.

These data agree with previous literature reports, which stressed the importance of preparing the samples as a thin layer that permits evaporation of the blocking agent in order to regenerate the isocyanate,[89] and supports the possibility of carrying out blocking reactions at elevated temperatures. ^{1}H and ^{13}C NMR spectra of B-HDIT after heating at 180 °C for 1 h did not show significant changes with respect to the original compound.

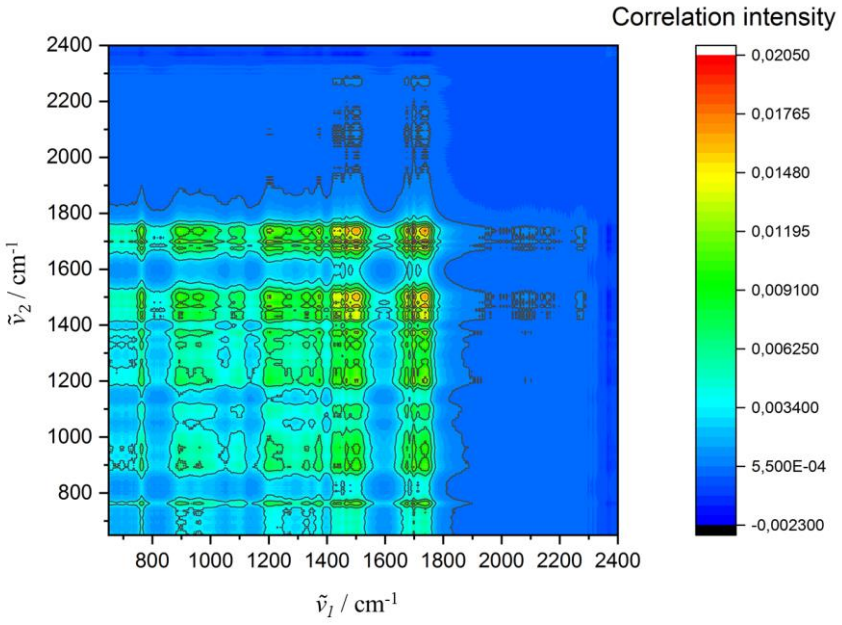

Figure 26. Synchronous 2D-IRcorr spectra for B-HDIT heated at 180 ºC for 1 h.

4.3. Preliminary Batch Experiments

The exothermic reaction between HDIT and MEKO releases 190 kJ per kilogram of material.[95] To estimate the reaction time between HDIT and MEKO required to obtain full conversion and to evaluate the temperature overshoot produced by the reaction exotherm, a series of preliminary batch experiments were performed in a three-necked round bottom flask. All initial batch reactions were carried out on 35 mmol scales. HDIT was initially placed in the flask and agitated using a mechanical stirrer, which was situated vertically in the flask (appropriate mixing of the viscous material could not be achieved using a magnetic stirrer). The IR probe was located in one of the lateral necks of the flask, with an angle of approximately 25° with respect to the vertical mechanical stirrer (Figure 15). FT-IR spectra and temperature data were collected in intervals of 15 s. The starting material was preheated to several starting temperatures, ranging from 28 °C to 74 °C. 1 mol % of dibutyltin dilaurate was added as a catalyst in some of the experiments for comparison purposes. When the starting material reached the desired temperature, MEKO was added as fast as possible via syringe. The amount of MEKO utilized corresponded to a stoichiometry 1:1 with respect to the isocyanate content of the starting material. Selected results of the reaction monitoring are collected in Figure 27. Shortly upon addition of MEKO (addition of the reagent is marked

with an arrow in Figure 27), a strong temperature increase of > 50 °C was observed in all cases, accompanied by a rapid drop of the isocyanate IR signal. Rapid reactions and a sharp temperature increase of ca. 60 °C were observed at room temperature, both with and without the addition of dibutyltin dilaurate as catalyst (Figures 27a and 27b). The reaction is therefore very fast in the absence of additives even without preheating of the starting materials. As expected, the final temperature provoked by the reaction exotherm increased with the initial temperature of the sample (Figures 27c and 27d). Preheating the reaction vessel at 75 °C (the target temperature for the HDIT feed under continuous flow conditions, *vide infra*), the reaction reached 130 °C. After the initial rapid drop of the NCO signal (over 10–20 s), the signal decrease became slower (Figures 27a–d). Full reaction conversion (< 1 % NCO) was achieved in less than 2 min in all cases. The colorless reaction mixtures obtained contained analytically pure B-HDIT (IR and NMR analysis) in quantitative yield.

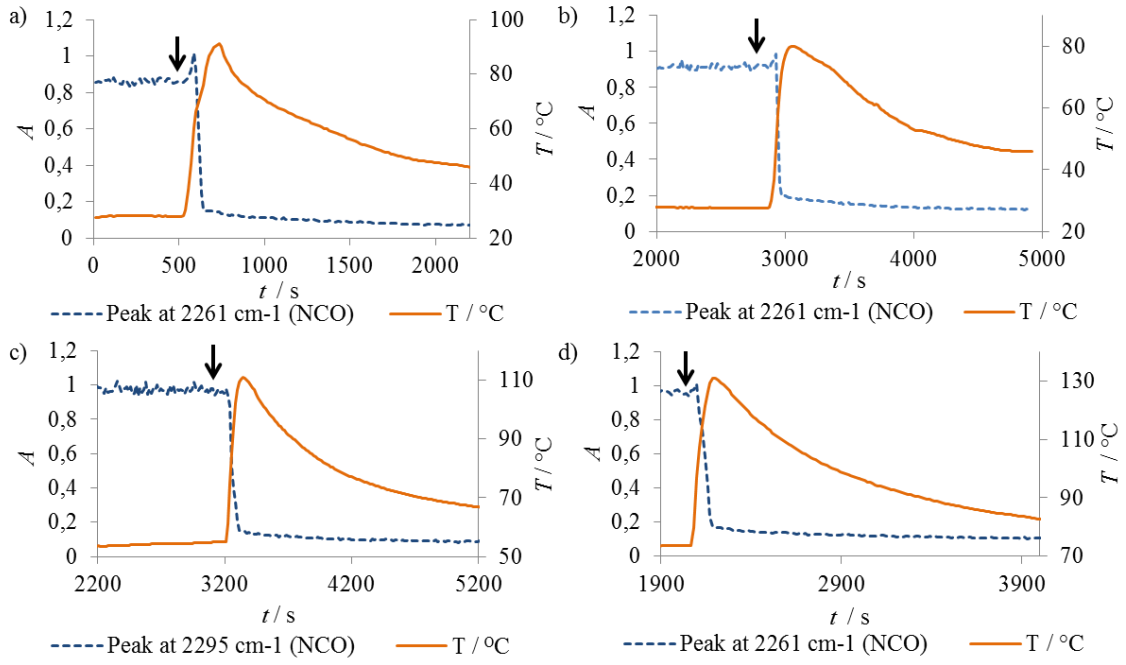

Figure 27. Monitoring of the reaction progress (NCO band at 2261 cm^{-1}) and temperature during the addition of MEKO to HDIT: a) at 28 °C, b) at 28 °C with dibutyltin dilaurate as an additive, c) at 54 °C, d) at 74 °C. Addition of MEKO is marked with a black arrow.

The high temperatures attained by self-heating of the reaction mixture due to the exothermic carbamate formation, even at very small scale (ca. 18 g), stressed the problems associated with temperature control for this process in batch. Furthermore, mixing of the reaction also proved troublesome. The high viscosity of the starting material (ca. 3000 mPa s

at 25 °C) made appropriate stirring at room temperature difficult. Preheating of HDIT reduced its viscosity and facilitated stirring, but aggravated the temperature overshoot. As mentioned above, large scale preparation of B-HDIT requires slow addition of the reactants over several hours to avoid overheating. Yet, the factual reaction time is as short as 2 min at moderate temperatures (Figure 27). Efficient control of the reaction temperature via heat transfer intensification, therefore, has the potential to overcome these limitations and to provide higher productivities and a fully scalable solution. With this in mind, we developed a continuous flow procedure for the preparation of B-HDIT.

4.4. Continuous Flow Preparation of B-HDIT and Process Intensification

Batch experiments revealed that the isocyanate reacts very fast with MEKO (< 2 min) and that the main challenges for the process are to achieve appropriate mixing and temperature control. The design of the flow reactor, therefore, focused initially on the proper mixing of the two neat reactants. The continuous flow setup consisted of two feeds containing neat HDIT and MEKO (Figure 28a). MEKO (ca. 15 mPa s at 20 °C)[95] was pumped using a standard syringe pump. Accurate dosing of the highly viscous HDIT (ca. 3000 mPa s at 25 °C) was difficult to achieve using standard laboratory-scale pumping units. The liquid could be satisfactorily pumped using a peristaltic pump modified with a special pumping head to handle viscous systems (Vapourtec SF10) and preheating the starting material to 75 ºC. By heating the HDIT feed, the viscosity is reduced from ca. 3000 mPa s to < 500 mPa s (see Figure S7). Using this setup, the error in dosing HDIT was below 5 % (Figure S8), as determined by the weight of HDIT pumped over time. The experimental error was additionally utilized to calibrate the pump, resulting in perfect dosing of the reactant. The streams were mixed using a modified Y-connector and a mixing unit (3 mm diameter Kenics mixers, 980 µL dead volume) (Figure 28b). The Y-connector was tailored to enable injection of MEKO directly into the center of the HDIT stream (Figure 28c). This configuration has been shown as optimal for mixing of liquid streams in some cases.[96,97] The modified Y-connector provided excellent mixing within the Kenics mixer and allowed for a significantly reduced length of the mixing unit. The homogeneous reaction mixture obtained after the mixing unit entered a residence time unit consisting of PFA tubing (3.2 mm i.d., 4.8 mm o.d.), thermostated with a heating jacket controlled by a Huber thermostat. The temperature was additionally monitored with two thermocouples (one at the input of thermal fluid and one at

the output). From the average value of the two temperatures, a correction factor was calculated for the temperature drop and used for the setting of the thermostat temperature, to ensure that the average value of the reactor temperature is at the desired point. The FT-IR probe was connected to the reactor output via a T-junction. The probe was connected linearly with the reactor output so that the reaction streams made a 90° turn in front of the IR probe ensuring good mixing at the monitoring point (see Figure 17). An additional challenge of the continuous flow process was the very high viscosity of the target compound B-HDIT (over 100 000 mPa s at 25 °C, Figure S8), which could cause an important pressure drop and blockage of the reactor. To overcome this issue the non-thermostated tubing at the reactor output was kept very short (ca. 2 cm) (Figure 17). In this manner, the viscous fluid obtained at the reactor output was still hot enough to have moderate viscosity and prevent clogging of the system.

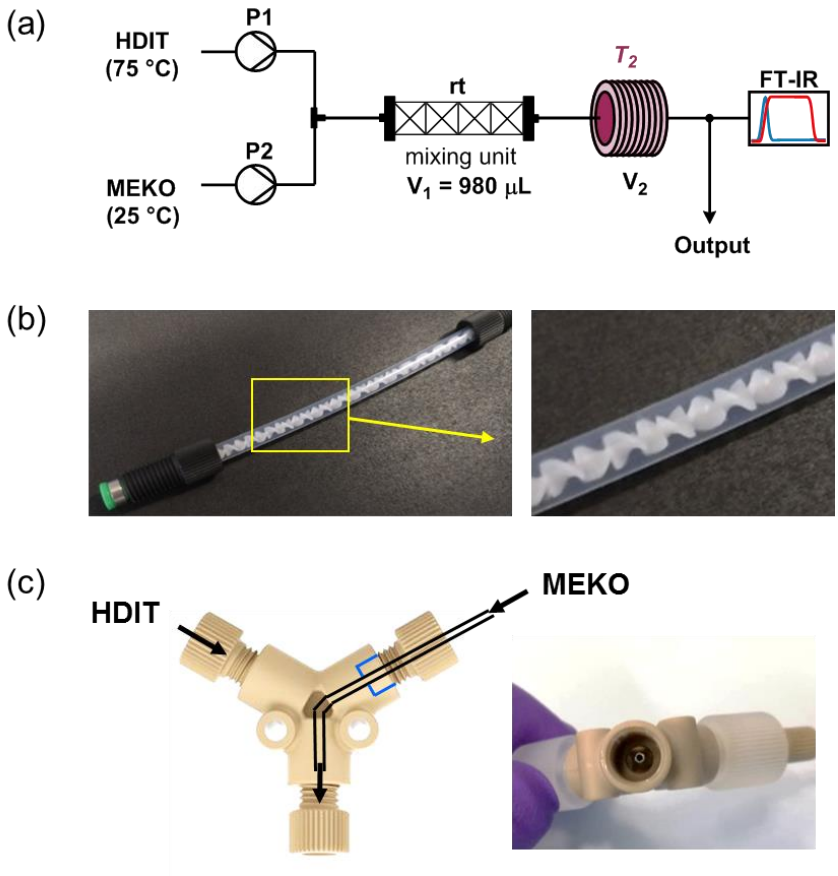

Figure 28. a) Schematic view of the continuous flow setup utilized for the synthesis of B-HDIT. b) Static mixer-containing tube (i.d. 3 mm, length 12.5 cm) utilized as a mixing unit. c) Schematic drawing an image of the modified Y-connector for the direct injection of MEKO into the center of the HDIT stream.

Initial flow experiments were conducted using a temperature of 100 ºC and an internal volume of 14.65 mL for the residence time unit (V_2 and T_2, Figure 28a). The temperature of the mixing unit V_1 was not regulated (contact with air at ambient conditions). The flow rate of the neat reactants was set to 1.00 mL min^{-1} and 1.74 mL min^{-1} for MEKO and HDIT, respectively (0.923 g min^{-1} of MEKO and 2.035 g min^{-1} of HDIT). In a typical experiment, only HDIT was initially pumped. As soon as the MEKO feed was switched on, and after the corresponding residence time (ca. 5.7 min) had passed, the NCO signal rapidly dropped to 0 % (Figure 29) and remained stable at this value, indicating full conversion to the target product B-HDIT.

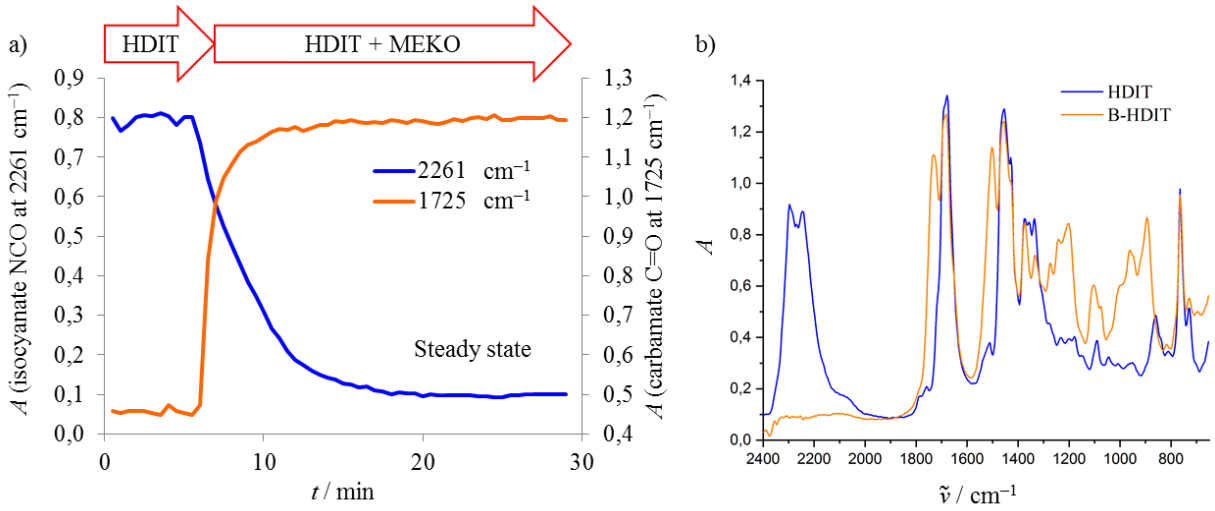

Figure 29. a) *In-line* IR monitoring of the reaction under continuous flow conditions. b) Comparison of the IR spectra measured for HDIT and the output of the reactor stream.

Next was to evaluate the continuous flow blocking reaction under intensified conditions. Keeping the temperature (100 °C) constant for the 14.65 mL residence time unit (V_2), the total flow rate was gradually increased from 2.74 mL min^{-1} to 14.10 mL min^{-1}, resulting in a residence time decrease from 5.35 min to 1.04 min in the heated residence time unit (5.7 min and 1.11 min in total including the mixing zone). Full conversion to the desired B-HDIT compound (with 0 % NCO being detected by FT-IR) was obtained in all cases. Notably, a temperature gradient could be observed along the length of the mixing unit by thermal imaging (Figure S10). Accurate temperature measurements using a thermocouple at the inlet and outlet of the mixing unit revealed that the HDIT stream enters the system at

65 °C (the temperature of the heated liquid feed decreases from 75 °C to 65 °C). Due to mixing with MEKO the temperature of the mixture decreased slightly and then increased again due to the reaction exotherm, reaching 87 ºC at the reactor outlet. Using a shorter residence time unit V_2 (3.5 mL volume) the reaction time could be further reduced to 45 s without the complete conversion at 100 °C (10 % NCO). At 115 °C complete conversion was observed using residence time of 45 s but further decrease in residence time resulted in increase in NCO content. The stepwise increase of the reaction temperature up to 155 °C enabled full conversion after 30 s residence time. The reaction time required to obtain full conversion could be additionally shortened to 15 s by heating the residence time unit to 155 °C (Figure 30). Under these conditions, 0 % NCO was detected by *in-line* FT-IR monitoring, which was additionally confirmed by ^{1}H and ^{13}C NMR spectra of samples collected from the reactor output.

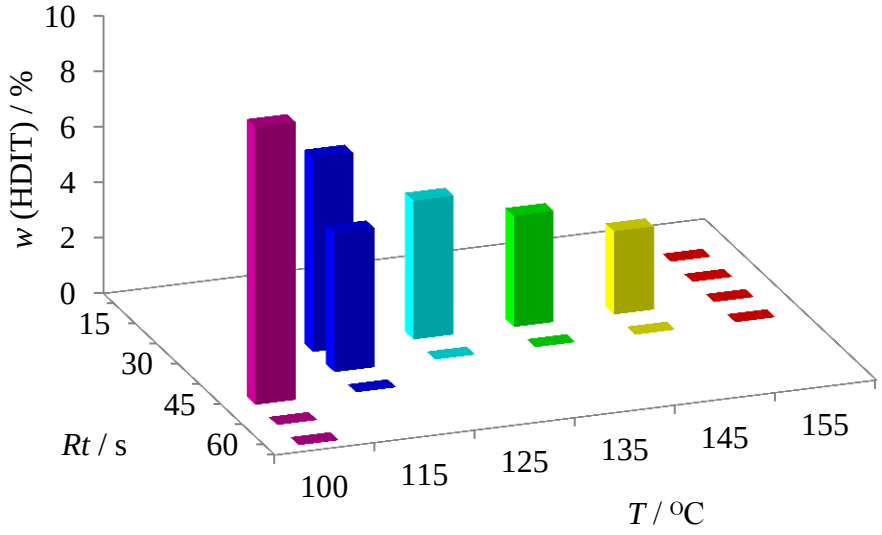

Figure 30. Intensification of the synthesis of B-HDIT under continuous flow conditions showing the percentage of NCO in reaction mixture based on absorption at 2261 cm^{-1} as a function of residence time and reaction temperature.

To assess the stability of the continuous flow process, the 15 s reaction at 155 ºC was executed for 3.5 h under the intensified conditions (Figure 18). *In-line* IR monitoring of the reaction showed a stable signal corresponding to 0 % NCO. The long run experiment resulted in 3.3. kg of pure B-HDIT (purity was confirmed by ^{1}H and ^{13}C NMR spectroscopy), which

corresponds to the productivity of nearly 1 kg h^{-1} for a reactor of only 4.5 mL (0.98 mL + 3.5 mL) volume. The space-time yield calculated for the process is 204 kg h^{-1} L^{-1}, superior to that obtained for a typical batch, stirred-tank based processes (< 0.1 kg h^{-1} L^{-1}).

5. CONCLUSION

In conclusion, we have developed a continuous flow, intensified procedure for the preparation of the blocked isocyanate B-HDIT from the HDI trimer and MEKO. *In-line* IR analysis was successfully implemented as a tool for monitoring the degree of disappearance of isocyanate during the formation of B-HDIT. The method could be used for quantitative purposes at conversions above 80 %. Batch experiments revealed that the blocking reaction is fast, highly exothermic, and difficult to scale due to the problems associated with the high amount of heat released and the highly viscous nature of the starting material. Utilization of additives such as dibutyltin dilaurate as catalyst proved unnecessary even when the reactants were mixed at room temperature. To achieve appropriate mixing of the viscous streams, a key factor to obtain clean and fast reactions in flow, a Kenics static mixer and concentric injection of MEKO to the isocyanate stream were utilized. Intensification of the process by gradually increasing the temperature and decreasing the reaction time permitted the preparation of the target compound after a residence time as short as 15 s at 155 °C. This corresponded to productivity of ca. 1 kg h^{-1} for a reactor with a volume of only 4.5 mL (0.98 mL mixing unit + 3.5 mL residence time). The reactor was stable under intensified conditions, and the reaction could be run uninterrupted for 3.5 h, yielding to 3.3 kg of pure material. Application of this methodology to large scale production will significantly increase the green chemistry metrics of the process, with reduced processing time and a much larger space-time yield. Moreover, the increased robustness of continuous production has enabled a reliable protocol that does not require the addition of heavy metal catalysts.

6. LIST OF ABBREVIATIONS AND SYMBOLS

1D – one-dimensional

2D – two-dimensional

2Dcorr – two-dimensional correlation spectroscopy

2D-IR – two-dimensional infrared spectroscopy

2D-IRcorr – two-dimensional infrared correlation spectroscopy

A – absorbance

A_h – heat transfer surface area

ATR – attenuated total reflection

B-HDIT – blocked hexamethylene diisocyanate

DSC – differential scanning calorimetry

FT-IR – Fourier transform infrared spectroscopy

HBA – hydrogen bond acceptor

HBD – hydrogen bond donor

HDI – hexamethylene diisocyanate

HDIT – hexamethylene diisocyanate trimer

i.d. – internal diameter

IR – infrared

LOD – limit of detection

LOQ – limit of quantification

MEKO – methyl ethyl ketoxime

o.d. – outer diameter

^{o}C – degree celsius

P_1 – first pump

P_2 – second pump

PAT – process analytical technologies

PFA – perfluoroalkoxy

Pr_1 – product

Pr_2 – side product

Q – heat flux

q – heat transfer rate

Re – Reynolds number

Rt – residence time

rt – room temperature

RTD – resistive temperature device

S_{bl} – signal intensity for the blank sample

S_m – minimal analyticaly distinguishable signal

T – temperature

t – time

T_1 – temperature of the first part of the flow reactor

T_2 – temperature of the second part of the flow reactor

TGA – termogravimetric analysis

$TMSN_3$ – trimethylsilyl azide

U – Heat transfer coefficient

UV-Vis – ultraviolet and visible spectroscopy

V_1 – internal volume of the first part of flow reactor

V_2 – internal volume of the second part of flow reactor

w – mass fraction

ΔT – difference in temperatures

ΔT_{LM} – Logarithmic mean temperature difference

$\Delta\Delta G^{\ddagger}$ – difference in transition state energies

$\tilde{\nu}$ – wavenumber axis in one dimensional infrared spectrum

$\tilde{\nu}_1$ – x-axis in two dimensional infrared correlation spectra

$\tilde{\nu}_2$ – y-axis in two dimensional infrared correlation spectra

σ_{bl} – standard deviation for blank sample

η – viscosity

7. REFERENCES

1. A. Austin, D. A. Hicks, *PU Magazine.* **14** (2017) 1–15.
2. Y. Camberlin, P. Michaud, C. Pesando, J. P. Pascault, *Makromol. Chem. Macromol. Symp.* **25** (1989) 91–99.
3. D. Levin, *ACS Symposium Series*. **2014** 1181 pp 3–71.
4. X. M. Zhong, I. Wyman, H. Yang, J. B. Wang, X. Wu, *Chem. Eng. J.* **302** (2016) 744–751.
5. I. Ahmad, J. H. Zaidi, R. Hussain, A. Munir, *Polym. Int.* **56** (2007) 1521–1529.
6. P. J. Driest, V. Lenzi, L. S. A. Marques, M. M. D. Ramos, D. J. Dijkstra, F. U. Richter, D. Stamatialis, D. W. Grijpma, *Polym. Adv. Technol.* **28** (2017) 1299–1304.
7. D. A. Wicksa, Z. W. Wicks, *Prog. Org. Coat.* **36** (1999) 148–172.
8. D. A. Wicksa, Z. W. Wicks, *Prog. Org. Coat.* **41** (2001) 1–83.
9. E. Delebecq, J. P. Pascault, B. Boutevin, F. Ganachaud, F. *Chem. Rev.* **113** (2013) 80-118.
10. M. S. Rolph, A. L. J. Markowska, C. N. Warriner, R. K. O'Reilly, *Polym. Chem.* **7** (2016) 7351–7364.
11. R. Gérardy, N. Emmanuel, T. Toupy, V. E. Kassin, N. N. Tshibalonza, M. Schmitz, J. C. M. Monbaliu, *Eur. J. Org. Chem.* **20-21** (2018) 2301–2351.
12. M. B. Plutschack, B. Pieber, K. Gilmore, P. H. Seeberger, *Chem. Rev.***117** (2017) 11796–11893.
13. I. R. Baxendale, L. Brocken, C. J. Mallia, *Green Proc. Synth.* **2** (2013) 211–230.
14. B. Gutmann, D. Cantillo, C. O. Kappe, *Angew. Chem. Int. Ed.* **54** (2015) 6688–6728.
15. K. F. Jensen, B. J. Reizmana, S. G. Newman, *Lab. Chip.* **14** (2014) 3206–3212.
16. T. Jamison, G. Koch, *Science of Synthesis: Flow Chemistry in Organic Synthesis*, Georg Thieme Verlag KG, Stuttgart, Germany, 2018.
17. F. Darvas, V. Hessel, G. Dorman, *Flow Chemistry*, De Gruyter, Berlin, 2014.
18. W. Reschetilowski, *Microreactors in Preparative Chemistry*, Wiley-VCH, Weinheim, 2013.
19. Wirth, *Microreactors in Organic Synthesis and Catalysis, 2nd Ed.*, Wiley-VCH, Weinheim, 2013.

20. M. A. Marsini, F. G. Buono, J. C. Lorenz, B. Yang, J. T. Reeves, K. Sidhu, M. Sarvestani, Z. Tan, Y. Zhang, N. Li, H. Lee, J. Brazzillo, L. J. Nummy, J. C. Chung, I. K. Luvaga, B. A. Narayanan, X. Wei, J. J. Song, F. Roschangar, N. K. Yee, C. H. Senanayake, *Green Chem.* **19** (2017) 1454–1461.
21. L. Rumi, C. Pfleger, P. Spurr, U. Klinkhammer, W. Bannwarth, *Org. Process Res. Dev.* **13** (2009) 747–750.
22. H. R. Sahoo, J. G. Kralj, K. F. Jensen, *Angew. Chem. Int. Ed.* **46** (2007) 5704–5708.
23. C. R. Sagandira, P. Watts, *Eur. J. Org. Chem.* **44** (2017) 6554–6565.
24. P. K. A. Panandiker, D. E. Tweet, *Continuous Process for the Production of Blocked Isocyanates*, US Patent 4,055,551, 1977.
25. Viscosity data for **HDIT** were obtained from the MSDS of the commercial compound utilized: *DESMODUR N 3300*, Safety Data Sheet according to Regulation (EU) No. 1907/2006. MSDS No. 112000013102, https://www.productsafetyfirst.covestro.com. (date of access march 6th 2016).
26. Y. Park, I. Noda, Y. M. *Jung, Front. Chem*. **3** (2015) 1–16.
27. L. Malet-Sanz, F. Susanne, *J. Med. Chem.* **55** (2012) 4062–4098.
28. T. Wirth, *Microreactors in Organic Synthesis and Catalysis, 2nd ed*. Wiley-VCH, Weinheim, 2013.
29. V. Hessel, J. C. Schouten, A. Renken, Y. Wang, J.I. Yoshida, *Handbook of Micro Reactors*, Wiley-VCH, Weinheim, 2009.
30. E. L. Paul, V. A. Atiemo-Obeng, S. M. Kresta, *Handbook of Industrial Mixing: Science and Practice;* John Wiley & Sons, 2004; pp 1385.
31. A. Ghanem, T. Lemenand, D. D. Velle, H. Peerhossainic, *Chem. Eng. Res. Des.* **92** (2014) 205–228.
32. D. J. Lamberto, M. M. Alvarez, F. J. Muzzio, *Chem. Eng. Sci.* **54** (1999) 919−942.
33. J. i. Yoshida, *Chem. Commun*. (2005) 4509−4516.
34. G. A. Price, D. Mallik, M. G. Organ, *J. Flow Chem.* **7** (2017) 82–86.
35. M. Baumann, *Org. Biomol. Chem.* **16** (2018) 5946–5954.
36. K. A. Bakeev, *Process Analytical Technology – Spectroscopic Tools and Implementation Strategies*, John Wiley & Sons, 2nd edn., 2010.
37. E. Buchner, T. Curtius, *Chem. Ber*. **18** (1885) 2371–2377
38. T. Curtius, *J. Prakt. Chem*. **125** (1930) 303–424.

39. A. W. Hoffman, *Ber.* **14** (1881) 2725–2736.
40. A. W. Hoffman, *Ber.* **15** (1882) 407–416.
41. A. W. Hoffman, *Ber.* **15** (1882) 762–775.
42. A. W. Hoffman, *Ber.* **17** (1884) 1406–1412.
43. E. Ware, Chem. Rev. **46** (1950) 403–470.
44. W. Lossen, *Liebigs Ann. Chem*. **150** (1869) 313–325.
45. W. Lossen, *Liebigs Ann. Chem*. **175** (1872) 271.
46. W. Lossen, *Liebigs Ann. Chem*. **161** (1872) 347–362.
47. *G. Bertrand, J. Majoral, A. Baceiredo, Tetrahedron Lett. **21** (1980) 5015–5018.*
48. L. Kurti, B. Czako, *Strategic applications of named reaction in organic synthesis, Background and Detailed mechanisms,* Elsevier Academic Press, 2005, Pages: 116–117, 210–211, 266–267.
49. J. J. Li, *Name reactions, A collection of detailed Mechanisms and Synthetis Applications, Fifth edition,* Springer International Publishing, 2014. Page 367.
50. M. F. Sonnenschein, *Polyurethanes: Science, Technology, Markets, and Trends*, John Wiley and Sons, Hoboken, New Jersey, 2015.
51. K. Ashida, *Polyurethane and Related Foams: Chemistry and Technology*, CRC Taylor and Francis, Boca Raton, Florida, 2006.
52. U. Meier-Westhues, *Polyurethanes: Coatings, Adhesives and Sealants*, Vincentz Network, Hannover, Germany, 2007.
53. J. A. Bridson, *Plastics Materials Seventh Edition*, Elsevier, 1999, Pages 778–809.
54. F. Richter, Isocyanates, *Ullmann's Encyclopedia of Industrial Chemistry*, Wiley-VCH Verlag, Weinheim, Germany, 2011.
55. S. Petersen, *Liebigs Ann. Chem.* **562** (1949) 205–228.
56. P. Krol, J. Wojturska, *J. Appl. Polym. Sci.* **88** (2003) 327–336.
57. C. Dubois, S. Désilets, A. Ait-Kadi, P. Tanguy, P., *J. Appl. Polym. Sci.* **58** (1995) 827–834.
58. B. Grepinet, F. Pla, P. Hobbes, P. Swaels, T. Monge, *J. Appl. Polym. Sci.* **75** (2000) 705–712.
59. J. M. Lee, S. Subramani, Y. S. Lee, J. H. Kim, *Macromol. Res.* **13** (2005) 427–434.
60. H. Kothandaraman, R. Thangavel, *J. Appl. Polym. Sci.* **47** (1993) 1791–1796.
61. S. Subramani, Y. J. Park, Y. S. Lee, J. H. Kim, *Prog. Org. Coat.* **48** (2003) 71–79.

62. C.N. Bamwell, *Fundamentals of Molecular Spectroscopy,* third edition, McGraw-Hill London, 1983, pages 1–9.

63. P. Larkin, *Infrared and Raman Spectroscopy – Principles and Spectral Interpretation,* Elsevier, Walthman MA, USA, 2011, pages 27–31.

64. Y. Marechal, *The Hydrogen Bond and the Water Molecule, The Physics and Chemistry of Water, Aqueous and Bio Media*, Elsevier, Amsterdam, 2007, pages 77-111

65. G. Socrates, *Infrared and Raman Characteristic Group Frequencies Tables and Charts Third Edition,* John Wiley and Sons, Chichester, 2001, pages 78–150.

66. J. Gironès, M. T. B. Pimenta, F. Vilaseca, A. J. F. de-Carvalho, P. Mutjé, A. A. S. Curvelo, *Carbohydr. Polym.* **68** (2007) 537–543.

67. M. Cho, *Chem. Rev.* **108** (2008) 1331–1418.

68. Y. Park, I. Noda, Y. M. Jung, *J. Mol. Struct.* **1124** (2016) 11–28.

69. I. Noda, *J. Mol. Struct*. **1069** (2014) 3–22.

70. I. Noda, *J. Mol. Struct.* **1069** (2014) 23–49.

71. I. Noda, *J. Mol. Struct.* **1124** (2016) 3–7.

72. I. Noda, *J. Mol. Struct.* **1124** (2016) 29–41.

73. S. Morita, H. Shinzawa, I. Noda, Y. Ozaki, *J. Mol. Struct.* **799** (2006) 16–22.

74. I. Noda, Y. Ozaki, *Two-dimensional Correlation Spectroscopy – Applications in Vibrational and Optical Spectroscop,* John Wiley & Sons, Chichester, 2004, page 57–64.

75. I. Noda, A. E. Dowrey, C. Marcott, G. M. Story, Y. Ozaki, *Appl. Spectrosc*. **54** (2000) 236–248.

76. I. Noda, Y. Liu, Y. Ozaki, *J. Phys. Chem*. **100** (1996) 8665–8673.

77. H. Huang, S. Malkov, M. M. Coleman, P. C. Painter, *J. Phys. Chem. A.* **107** (2003) 7697–7783.

78. S. Šašić, A. Muszynski, Y. Ozaki, *J. Phys. Chem*. **104** (2000) 6380–6387.

79. S. Šašić, A. Muszynski, Y. Ozaki, *J. Phys. Chem*. **104** (2000) 6388–6394.

80. V. G. Gregoriou, J. L. Chao, H. Toriumi, R. A. Palmer, *Chem. Phys. Lett.* **179** (1991) 491–496.

81. I. Noda, G. M. Story, C. Marcott, *Vib. Spectrosc.* **19** (1999) 461–465.

82. Y. Ozaki, Y. Liu, I. Noda, *Macromolecules.* **30** (1997) 2391–2399.

83. Y. Ren, M. Shimoyama, T. Ninomiya, K. Matsukawa, H. Inoue, I. Noda, Y. Ozaki, *Appl. Spectrosc.* **53** (1999) 919–926.
84. F. Kimura, M. Komatsu, T. Kimura, *Appl. Spectrosc.* **54** (2000) 974–977.
85. A. Matsushita, Y. Ren., K. Matsukawa, H. Inoue, Y. Minami, I. Noda, Y. Ozaki, *Vib. Spectrosc.* **24** (2000) 171–180.
86. C. Li, J. Liu, J. Li, F. S, Q. Huang, H. Xu, *Polymer.* **53** (2012) 5423–5435.
87. I. Reva, L. Lapinski, R. Fausto, *J. Mol. Struct.* **976** (2010) 333–341.
88. J. Yenagi, A. R. Nandurkar, J. Tonannavar, *Spectrochim. Acta. A Mol. Biomol. Spectrosc.* **91** (2012) 261– 268.
89. D. A. Wicks, Z. W. Wicks, *Prog. Org. Coat.* **43** (2001) 131–140.
90. Q. W. Lu, T. R. Hoye, C. W. Macosko, *J. Polym. Sci. Part A: Polym. Chem.* **40** (2002) 2310–2328.
91. T. Shen, D. Zhou, L. Liang, J. Zheng, Y. Lan, M. Lu, *J. Appl. Polym. Sci.* **122** (2011) 748–757.
92. *2Dshige*(c) Shigeaki Morita, Kwansei-Gakuin University, 2004–2005.
93. W. John, J. Ledbetter, *J. Phys. Chem.* **81** (1977) 54–59.
94. The exotherm was measured by adiabatic calorimetry using a Vent Size Package (VSP) calorimeter using a closed stainless steel vessel under air atmosphere.
95. Viscosity data are included in the MSDS: 2-Butanone oxime, Thermo Scientific, Cat No.AC403330000,https://www.fishersci.com/shop/msdsproxy?productName=AC403331000 (accessed Jan 25th 2019).
96. J. Z. Luo, G. W. Chu, Y. Luo, M. Arowo, B. C. Sun, J. F. Chen, *AIChE J.* **63** (2017) 2876–2887.
97. J. Z. Luo, Y. Luo, G. W. Chu, M. Arowo, Y. Xiang, B. C. Sun, J. F. Chen, *Chem. Eng. Sci.* **155** (2016) 386–396.

8. APPENDIX

Herein is presented the additional information which supplements the results and discussion.

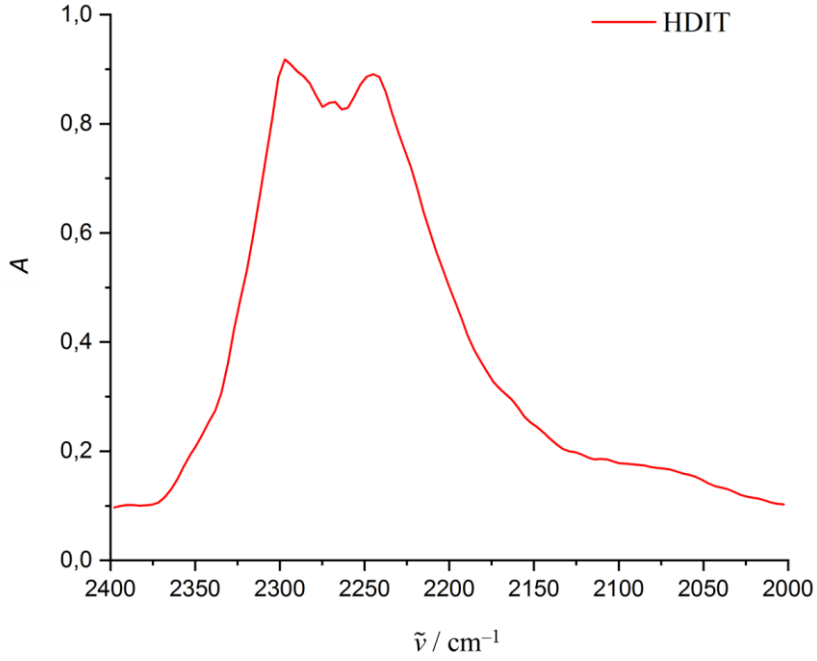

Figure S1. The isocyanate vibrational band in the IR spectrum of neat HDIT.

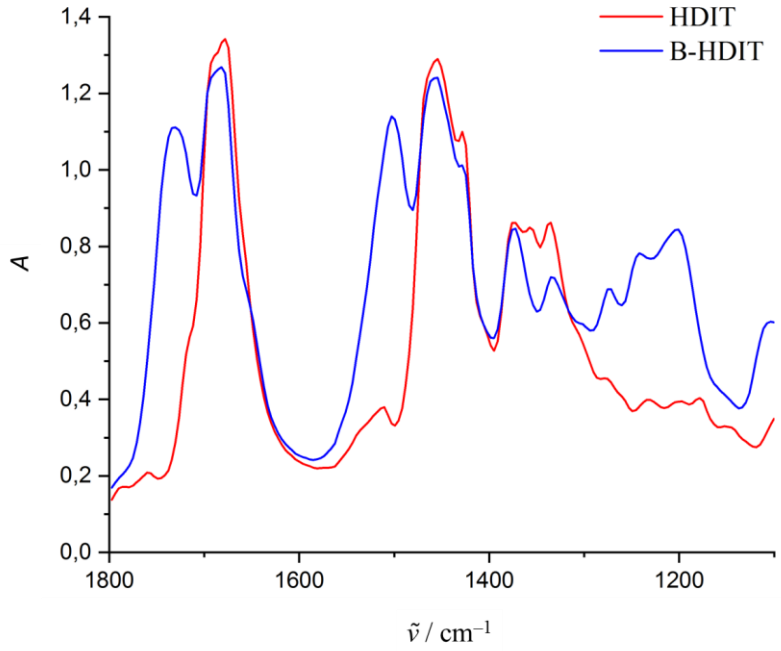

Figure S2. IR spectra of HDIT and B-HDIT in the range from 1800 cm^{-1} to 1100 cm^{-1}.

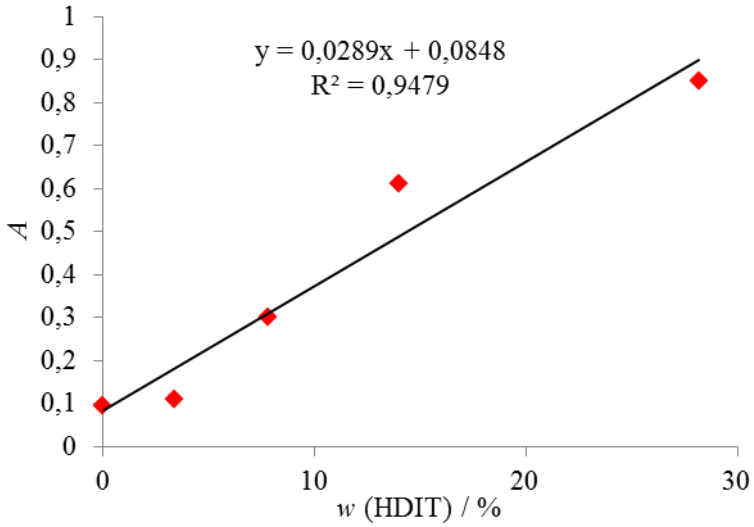

Figure S3. Calibration diagram of the NCO band absorption at 2261 cm^{-1} as a function of the content of HDIT from 0 to 30% in a mixture with its MEKO-blocked counterpart B-HDIT.

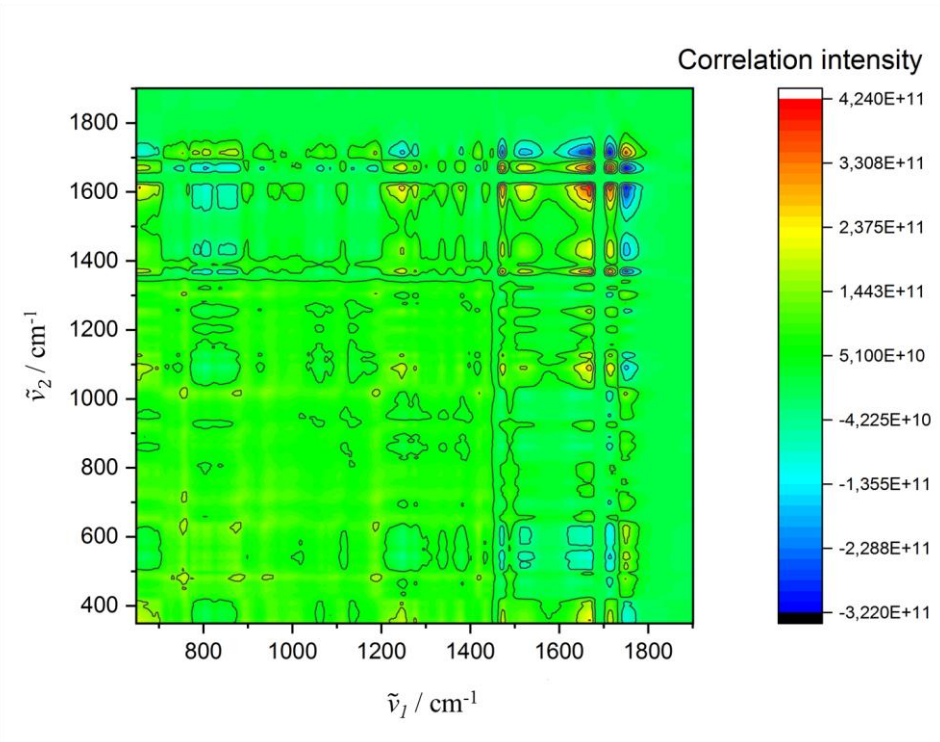

Figure S4. The synchronous 2D-IRcorr spectra for B-HDIT heated at a constant ramp of 8 °C min^{-1} from room temperature to 160 °C in the range from 650 cm^{-1} to 1900 cm^{-1}.

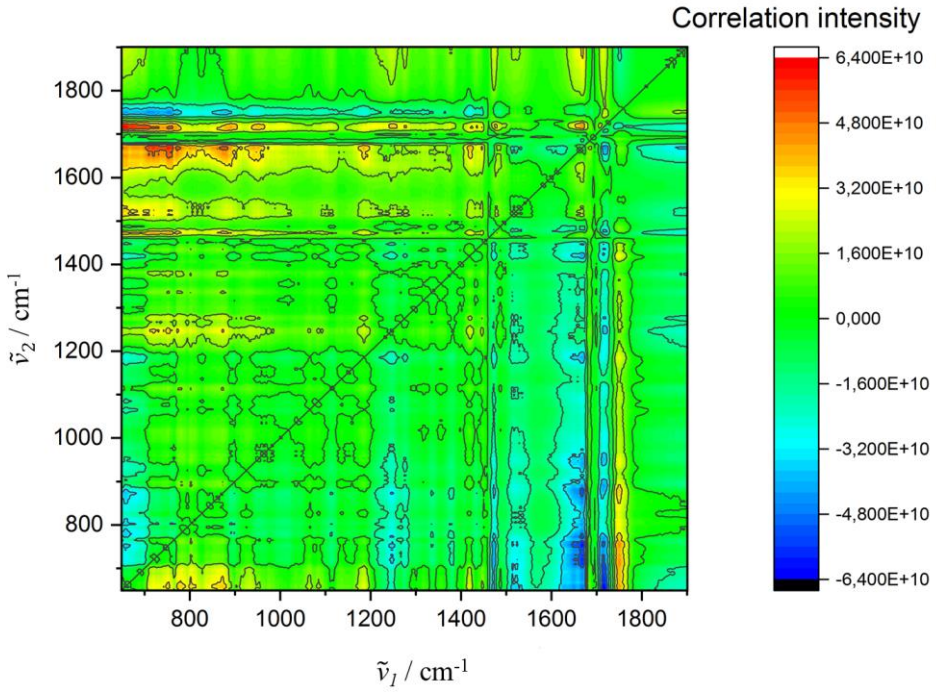

Figure S5. The asynchronous 2D-IRcorr spectra for B-HDIT heated at a constant ramp of 8 °C min^{-1} from room temperature to 160 °C in the range from 650 cm^{-1} to 1900 cm^{-1}.

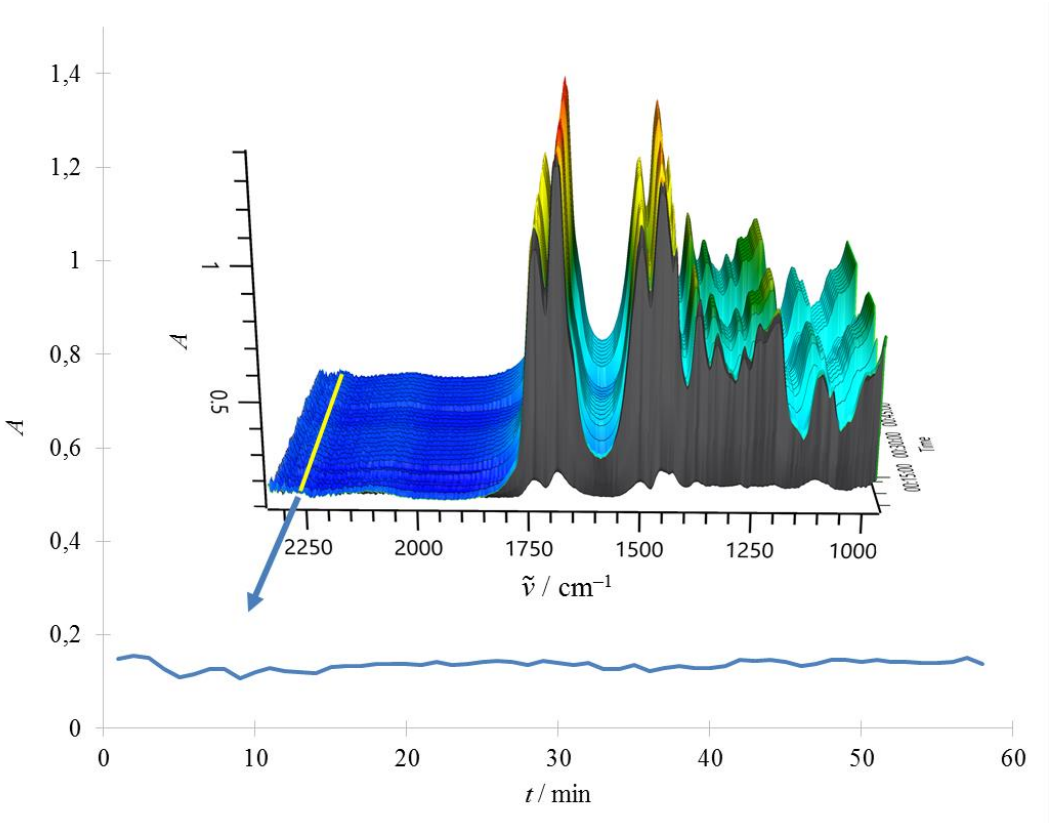

Figure S6. FT-IR monitoring of a B-HDIT sample heated at 180 °C for 1 h.

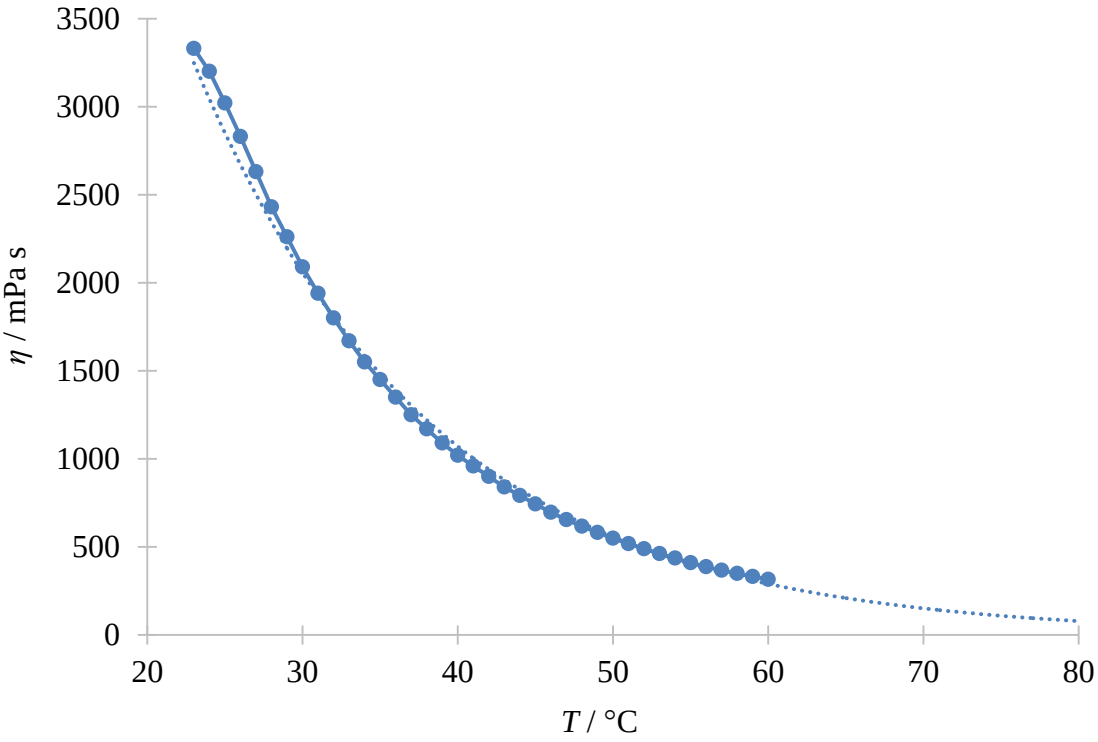

Figure S7. The viscosity of HDIT at different temperatures.

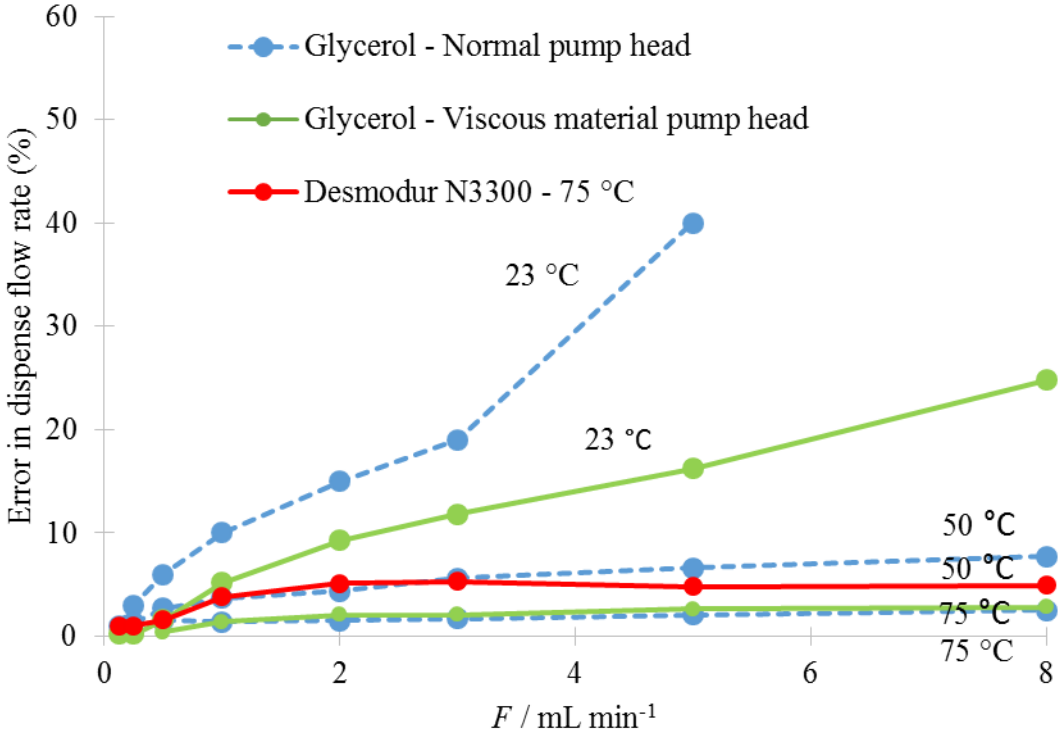

Figure S8. Performance of the Vapourtec SF10 pump equipped with a viscous solvent kit for glycerol (1000 mPa s) at different temperatures and HDIT (3000 mPa s) at 75 °C.

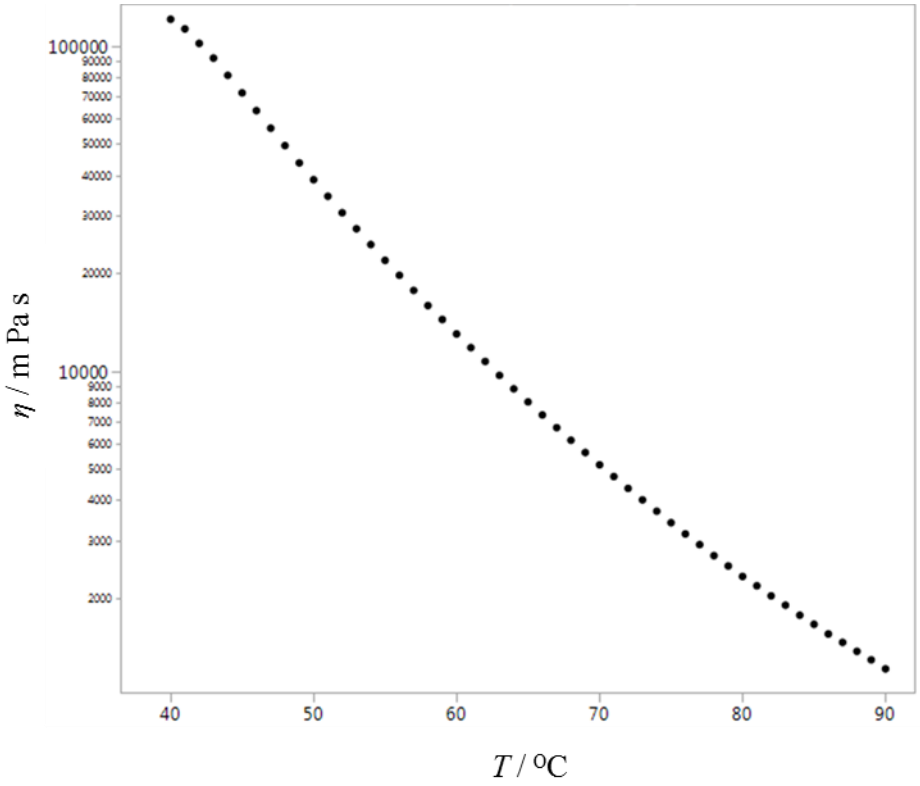

Figure S9. The viscosity of B-HDIT at different temperatures.

a) b)

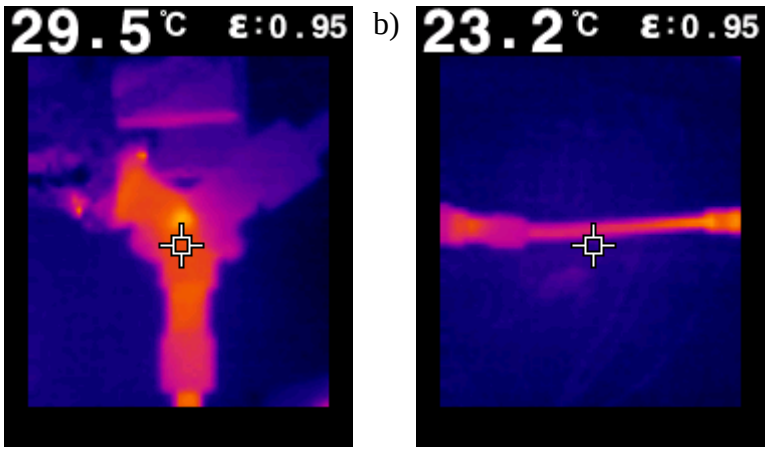

Figure S10. Thermal images of a) the Y connector and b) the Kenics mixer.

9. CURRICULUM VITAE

Personal Information

Name and surname: Gabriel Glotz

Date of birth: 20. January 1993

Place of birth: Nova Gradiška

Education

1999–2007	Mato Lovrak, Nova Gradiška
2007–2011	Veterinary school, Zagreb
2011–2014	Undergraduate study of Chemistry, Department of Chemistry, Josip Juraj Strossmayer University of Osijek, Osijek, Croatia.
2015	ERASMUS+ program, Institute of Analytical Chemistry and Food Chemistry, Graz University of Technology Graz, Austria
2017–	Graduate study of chemistry, research programme Analytical and Ogranic Chemistry, Department of Chemistry, Faculty of Sciences University of Zagreb, Zagreb Croatia,

Honours and Awards

2015	University Rector award, J. J. Strossmayer University of Osijek, Osijek, Croatia.
2015	2nd place on contest for the best student paper written. 5th Croatian and 1st International scientific and professional conference Water for all. J.J. Strossmayer University of Osijek, Croatia

Participation at Scientific Meetings and Conferences

1. G. Glotz, B. Gutmann, P. Hanselmann, A. Kulesza, D. Roberge, C. O. Kappe, Continuous Flow Synthesis of Indoles by Pd-catalyzed Deoxygenation of 2-Nitrostilbenes with Carbon Monoxide, 26th International Society of Heterocyclic

Chemistry Congress, September 3-8, 2015 Regensburg, Bavaria, Germany. Book of abstracts page 345.

2. G. Glotz, C. O. Kappe, Design and Construction of an Open Source-Based Photometer and its Applications in Flow Chemistry, 9th annual Flow Chemistry Europe 2019, February 26th – 27th 2019, Hinxton, Cambridge, UK

Scientific Publications

1. G. Glotz, C. O. Kappe, *React. Chem. Eng.* **3** (2018) 478–486.
2. B. Gutmann, M. Köckinger, G. Glotz, T. Ciaglia, E. Slama, M. Zadravec, S. Pfanner, M. C. Maier, H. Gruber-Wölfler, C. O. Kappe, *React. Chem. Eng.* **2** (2017) 919–927.
3. G. Glotz, R. Lebl, D. Dallinger, C. O. Kappe, *Angew. Chem. Int. Ed.*, ***56*** (2017) 13786–13789.
4. *G.* Glotz, D. Knoechel, P. Podmore, H. Gruber-Woelfler, C. O. Kappe, *Org. Process Res. Dev.* **21** (2017) 763–770.
5. G. Glotz, B. Gutmann, P. Hanselmann, A. Kulesza, D. Roberge, C. O. Kappe, *RSC Adv.* **7** (2017) 10469–10478.
6. D. Obermayer, D. Znidar, G. Glotz, A. Stadler, D. Dallinger, C. O. Kappe, *J. Org. Chem.* **81** (2016) 11788–11801.